# ERBB3 mediates the PI3K/AKT/mTOR pathway to alter the epithelial-mesenchymal transition in cervical cancer and predict immunity filtration outcome

XIAOYUE YANG  and  WEIPEI ZHU

Department of Obstetrics and Gynecology, The Second Affiliated Hospital of Soochow University,
Suzhou, Jiangsu 215000, P.R. China

**Abstract.** Cervical cancer is the fourth most common cancer among women worldwide, and the prognosis of advanced/recurrent cervical cancer remains poor. Metastasis and invasion of this type of cancer are closely associated with the tumor microenvironment. Studying the complex interactions between tumor progression and immune cells or stromal cells can provide new insights into treatment for patients with aggressive tumor, recurrence and drug resistance. In the present study, a bioinformatics method (Gene Expression Profiling Interactive Analysis, differentially expressed genes, Gene Ontology, Kyoto Encyclopedia of Genes and Genomes, protein-protein interactions and survival analysis) was used to explore the mRNA and protein level discrepancy gene signature of ERBB3 via the PI3K/AKT/mTOR pathway from the speculation in immuno-oncology and experimental verification of different cervical cancer cell lines. The high expression of ERBB3 in cervical cancer tissues (especially HPV-positive and adenocarcinoma-related) promoted the activation of the PI3K/AKT/mTOR pathway. The increased expression of MMP9 changed the macrophage infiltration in the tumor microenvironment and affected prognosis of patients with cervical cancer. In conclusion, the present study identified 14 EMT-related genes and 30 genes involved in the PI3K/AKT/mTOR pathway in cervical cancer, and they might provide novel clues for future treatment. The MMP family may be a notable factor associated with tumor cells and immune cells.

*Correspondence to:* Professor Weipei Zhu, Department of Obstetrics and Gynecology, The Second Affiliated Hospital of Soochow University, 1055 Sanxiang Road, Suzhou, Jiangsu 215000, P.R. China
E-mail: zwp333xx@126.com

## Introduction

Cervical cancer is the most common malignant tumor of the female genital tract worldwide (1). Persistent high-risk human papillomavirus (HPV) oncoproteins E6 and E7 are the main pathogenic factors of cervical cancer (2). At the molecular level, the HPV E6 and E7 proteins directly activate Akt, and this pathway is further stimulated in cervical cancer cells by amplifications and mutations of the PI3K genes. As it has a key role in the control of HPV gene expression and development of cervical cancer, the PI3K/AKT/mammalian target of rapamycin (mTOR) pathway may have potential as a therapeutic target for cervical cancer (3-5).

The tumor microenvironment (TME) contains stromal cells and immune cells that shape cancer development and impact responses to tumor therapy (6). Cancer cell proliferation, angiogenesis and metastasis also contribute to the establishment of an immunosuppressive environment. These factors are associated with tumor progression and poor clinical outcomes (7,8). However, factors that contribute to immunosuppression in the TME are poorly defined.

Epithelial-mesenchymal transition (EMT) plays an important role in tumor development from initiation to metastasis. EMT contributes to the majority of the hallmarks of cancer and continues to be an attractive target for cancer therapy (9). Classical EMT is characterized by the phenotype change of epithelial cells to cells with mesenchymal properties, but EMT is also associated with multiple other molecular processes, including tumor immune evasion (10). Immunosuppression occurs as a direct consequence of the EMT program or develops through some additional, still-uncharacterized signaling channels (11).

The PI3K/AKT/mTOR pathway can promote migration and induce EMT in numerous types of tumors, including cervical cancer (8,12). EMT-related changes in the expression of various receptor tyrosine kinases (RTKs) (13) have been reported, although the proliferation and survival dependence of specific RTKs under different conditions remains to be fully elucidated. The expression of an EGFR family member-ERBB3 (14) is associated with the epithelial phenotype of the cell line and the sensitivity to EGFR inhibition. ERBB3 heterodimerizes (15) with additional EGFR family members after stimulation with

various ligands, including neuregulin (16). ERBB3 contains multiple binding sites for p85, which is the regulatory subunit of PI3K (17). This allows direct recruitment and activation of PI3K signals via ERBB3 (18). Although changes in ERBB3 expression have been observed, the functional consequences of these changes and the relationship with downstream signals after EMT (19) have not been fully described.

These targets involved in cervical cancer are not functionally exclusive; rather, they are intertwined and reciprocal, and together they form intricate TME networks to meet context-specific needs for cellular function. To improve understanding of the correlation between TME and prognosis of cervical cancer, the present study assessed cervical cancer cell lines and tissues to reveal the roles of ERBB3 in the EMT induction of TME harboring immunosuppression, migration and invasion of cervical cancer, and to explore whether PI3K/AKT/mTOR signaling is involved in this process.

The current study intended to explore how ERBB3 mediates the PI3K/AKT/mTOR pathway and changes the tumor immune microenvironment to affect the EMT status of cervical cancer, which may provide further understanding of MMPs involved in immunotherapy.

## Materials and methods

*Data collection and preprocessing.* RNAseq data in the transcripts per million (TPM) format from The Cancer Genome Atlas (TCGA) (https://portal.gdc.cancer.gov/) and The Genotype-Tissue Expression (GTEx) (https://gtexportal.org/) were uniformly processed using the Toil process (20). Through extraction of the cervical squamous cell carcinoma and endocervical adenocarcinoma (CESC) data in TCGA and corresponding normal tissue data in GTEx, the 306 cervical tumor samples were classified as the malignant group and the three samples adjacent to cancer from TCGA together with the 10 normal cervix tissues from GTEx were classified as the non-malignant group. The RNAseq data in TPM format were log2 transformed for expression comparison between samples.

*Related hub genes selection.* A total of 14 EMT-related genes were selected based on the article 'Guidelines and definitions for research on epithelial-mesenchymal transition' written by the EMT International Association (TEMTIA) in 2020 (21). When searching for pathway related genes, GeneCards (https://www.genecards.org/) was used; the key words 'PI3K/AKT' and 'PI3K/AKT/mTOR' were searched for and genes with a relevance score >4.0 were selected.

*Gene Expression Profiling Interactive Analysis (GEPIA).* GEPIA (http://gepia.cancer-pku.cn/index.html) is a user-friendly web portal for gene expression analysis based on TCGA and GTEx data. In the current study, expression analysis of ERBB3 was evaluated using the project ID of TCGA-CESC. In the module 'Expression DIY' of GEPIA, the expression of ERBB3 between pan-cancer and normal tissue samples was studied with the option of matching normal TCGA data and GTEx data (Fig. 1A).

*Differentially-expressed genes (DEGs).* Batch correction, normalization and difference analysis of RNA-seq data from

GSE63514, GSE9750, and GSE44001 were performed to screen for DEGs in CESC samples. GSE63514 (22), GSE9750 (23) and GSE44001 (24,25) were obtained from the NCBI Gene Expression Omnibus database (ncbi.nlm.nih.gov/geo). The GSE63514 dataset used the GPL570 [HG-U133 Plus 2] Affymetrix Human Genome U133 Plus 2.0 Array platform, which contained 28 cervical cancer tissue samples and 24 normal samples. The GSE9750 dataset used the GPL96 Affymetrix Human Genome U133A Array platform and included 33 cervical cancer tissue samples that were primarily marked by HPV16 or HPV18, and 21 normal cervical samples. The GSE44001 dataset used the GPL14951 Illumina HumanHT-12 WG-DASL V4.0 R2 expression beadchip, which contained 300 cervical cancer tissue samples. GSE63514 and GSE9750 were set as the reference group and GSE44001 as the test group, and the R software limma package was used to identify DEGs between the groups (26). A total of 13,473 DEGs, including 6,514 downregulated and 6,595 upregulated genes, were identified in cervical cancer. The results were visualized using R software (version 3.6.3) (statistical analysis and visualization) with the R package ggplot2 [version 3.3.3] (27) to generate a volcano plot (Fig. 1C), which identified important genes.

*Genomic alteration types and alteration frequency analysis.* Genomic alteration types (missense mutation with putative driver or unknown significance, amplification and no alterations) and alteration frequency of 14 EMT-associated genes and 30 PI3K/AKT/mTOR pathway-associated genes were obtained from the cBioPortal for Cancer Genomics (http://www.cbioportal.org), using the 'OncoPrint' module and 'Cancer Types Summary' module for visualization.

*Immune cell infiltration estimation.* For the immune infiltration analysis, transcriptome or other omics data was used to calculate the score of immune cells in the tissue through algorithms, and inferred the infiltration of immune cells in the tissue. Single-sample Gene Set Enrichment Analysis (GSEA) in immune infiltration, which uses the markers of each type of immune cells (28), was used as the gene set to calculate the enrichment of each type of immune cells in each sample.

*Gene Ontology (GO) Term and Kyoto Encyclopedia of Genes and Genomes (KEGG) pathway enrichment analysis and GSEA.* GO and KEGG (29,30) analyses were applied to explore the biological functions of target genes in CESC. GO analysis is a powerful bioinformatics tool to determine the biological processes (BPs), cellular components (CCs) and molecular functions (MFs) related to ERBB3. GSEA was utilized to investigate the potential mechanisms of ERBB3. GO, KEGG and GSEA were performed using the R (version 3.6.4) package ClusterProfiler (31). P<0.1 and q<0.2 were selected as the cut-off level.

*Protein interactions and biological processes.* The direct and indirect relationship between ERBB3 and 30 hub genes in the PI3K/AKT/mTOR signaling pathway were analyzed using the online tool STRING (https://string-db.org).

*Reverse transcription-quantitative PCR (RT-qPCR).* The MecDNA-HUtrC007Ce01 commercial chip (cat.

no. 8*R100-M-20190104; Shanghai Outdo Biotech Co., Ltd.) contains cDNA reverse transcribed from RNA extracted from six cervical cancer cell lines: CaSki, MS751, ME180, C33A, SiHa and HeLa. According to the manufacturer's instructions, qPCR was performed using SYBR® Premix Ex Taq™ II (Tli RNaseH Plus; RR820Q,; Takara Bio, Inc.). Briefly, following the addition of 20 µl qPCR MasterMix into each well, the Axigen PlateMax Ultraclear Sealing Film (UC-500) was used to seal the chip, and it was placed on ice for 15 min to fully dissolve the freeze-dried cDNA. The chip was then centrifuged at 1,750 x g for 3 min at a temperature ramping rate of 2°C/sec. qPCR was performed using a Roche LightCycler® 480II (Roche Diagnostics) with the following program: Initial denaturation (95°C, 30 sec); 40 cycles of denaturation (95°C, 5 sec), annealing (60°C , 30 sec) and elongation (95°C, 5 sec); final elongation (60°C, 1 min) and a final hold (60°C). The fold-change of gene expression was calculated using $2^{-(\Delta Cq\ \text{experimental group} - \Delta Cq\ \text{control group})}$ (32). β-actin was used as an internal control and primers are as follows: ERBB3 Forward, 5'-GACCCAGGTCTACGATGGGAA-3'; ERBB3 reverse, 5'-GTGAGCTGAGTCAAGCGAG-3'; human β-actin forward, 5'-GAAGAGCTACGAGCTGCCTGA-3'; human β-actin reverse, 5'-CAGACAGCACTGTGTTGGCG-3' (product length, 191 bp).

*Risk survival analysis.* Kaplan-Meier curves (33) can describe the survival status of each group of patients or the survival status of each group of experimental animals. The present study analyzed RNA-seq data from TCGA-CESC cohort (n=304) and selected the median as the cutoff value. Hazard ratio (HR) is defined as the ratio of the two risk rates. When HR is >1, the research object is a risk factor; when HR is <1, the research object is a protective factor; when HR=1, the research object has no effect on survival time. As an outcome index, overall survival (OS) refers to the time to death. The prognostic data come from a Cell article (34). Data filtering: control/normal (not all items have control/normal) were removed and clinical information was retained. For the. nomogram chart, on the basis of multifactor regression analysis, the ruler score was set to characterize the situation of each variable in the multifactor regression model, and finally the total score was calculated to predict the probability of event occurrence (35).

*Transcriptomics analysis.* The key regulators in the PI3K/AKT/mTOR pathway were searched using TRRUST (https://www.grnpedia.org/trrust/), a reliable, intuitive tool for human and mouse transcriptional regulatory networks (36).

*Statistical analysis.* Software R (version 3.6.3) (37) was used for statistical analysis and visualization. For differential analysis of single gene expression, the R package of ggplot2 (version 3.3.3) (38) was used for visualization. For multi-gene association analysis, we used the R package of igraph (version 1.2.6) (39) and ggraph package (version 2.0.5) (40). For GO-KEGG analysis and GSEA, the R package of ggplot2 and cluster Profiler package was used (33). Visualization of Kaplan-Meier OS analysis was based on the use of the R package of survminer (0.4.9 version) (41) and for statistical analysis of survival data the survival package (3.2-10 version) was used. Wilcoxon rank sum test was used to assess differences in gene expression. Spearman's rank correlation coefficient was used to assess the significance of correlations. The qPCR data are presented as the mean ± standard deviation of three experiments, and qPCR and RNA-seq data were analyzed using one-way ANOVA followed by Tukey's multiple comparison test. P<0.05 was considered to indicate a statistically significant difference.

## Results

*Genomics*

*ERBB3 single-gene DEG in CESC.* In the CESC group, the average level of the normal group was 3.598±1.642, while the average level of the tumor group was 5.539±0.902. The difference was statistically significant (P<0.001) (Fig. 1A). Closely associated genes to ERBB3 in the PI3K/AKT/mTOR pathway were PIK3CA, PIK3R2, PIK3R3, ATG13, MTOR, RICTOR, RHEB and GSK3B (Fig. 1B).

The total number of gene identifications (IDs) after removing the null value was 35,905. Among them, 1,706 IDs met the |log2(FC)|>2 and P<0.05 threshold. Under this threshold, there were 1,221 IDs with high expression (positive logFC) and 485 with low expression (negative logFC). The genes that met this threshold and were significantly associated with EMT included MMP3 and SNAI2 (downregulated genes), and KRT12 (upregulated gene) (Fig. 1C). The expression of seven hub genes in the PI3K/AKT/mTOR pathway were increased in cervical cancer: EIF4EBP1, GSK3B, HRAS, KRAS, NRAS, PIK3CB and PIK3R2 (Fig. 2).

Figs. 3 and 4 show the somatic variation pattern in cervical cancer. These schematics represented the distribution of the number of protein-altering somatic mutations and copy number variations in 607 samples of cervical cancer. The highest frequencies of mutations among the EMT-related genes were revealed in MMP3 (11%, including amplification, deep deletion and missense mutation); PIK3CA (37%, including amplification and missense mutation); and PTEN (11%, including deep deletion and truncating mutation). PIK3CA mutation status assesses the hotspot mutations of the PIK3CA gene (42).

*Selection of EMT-related genes with GO and KEGG analyses.* Among 30 PI3K/AKT/mTOR pathway-related genes, upregulated genes in cervical cancer were as follows: EIF4EBP1 (P<0.001), GSK3B (P<0.001), HRAS (P<0.001), KRAS (P<0.05), NRAS (P<0.001), PIK3CB (P<0.001), and PIK3R2 (P<0.001); downregulated genes included CDKN1B (P<0.001), FOXO1 (P<0.001), FOXO3 (P<0.001), GRB10 (P<0.001), FOXO4 (P<0.001), NOS3 (P<0.001), PIK3R1 (P<0.001), PTEN (P<0.001), TSC2 (P<0.001), ULK1 (P<0.001), ATG13 (P<0.05), RPTOR (P<0.05) and RICTOR (P<0.001). Therefore, it is of certain significance to study this pathway in relation to carcinogenesis and prognosis of cervical cancer (Fig. 2B-D).

It was revealed that in cervical cancer the ERBB3 gene was enriched in the PI3K/AKT signaling pathway (NES=-1.707, P=0.045, FDR=0.034; Fig. 5).

TWIST1, tight junction protein 1 (TJP1), MMP9, MMP3 and vimentin (VIM) (Fig. 6) with all annotated functional molecules were compared using hypergeometric distribution tests to determine which functional roles were involved in that
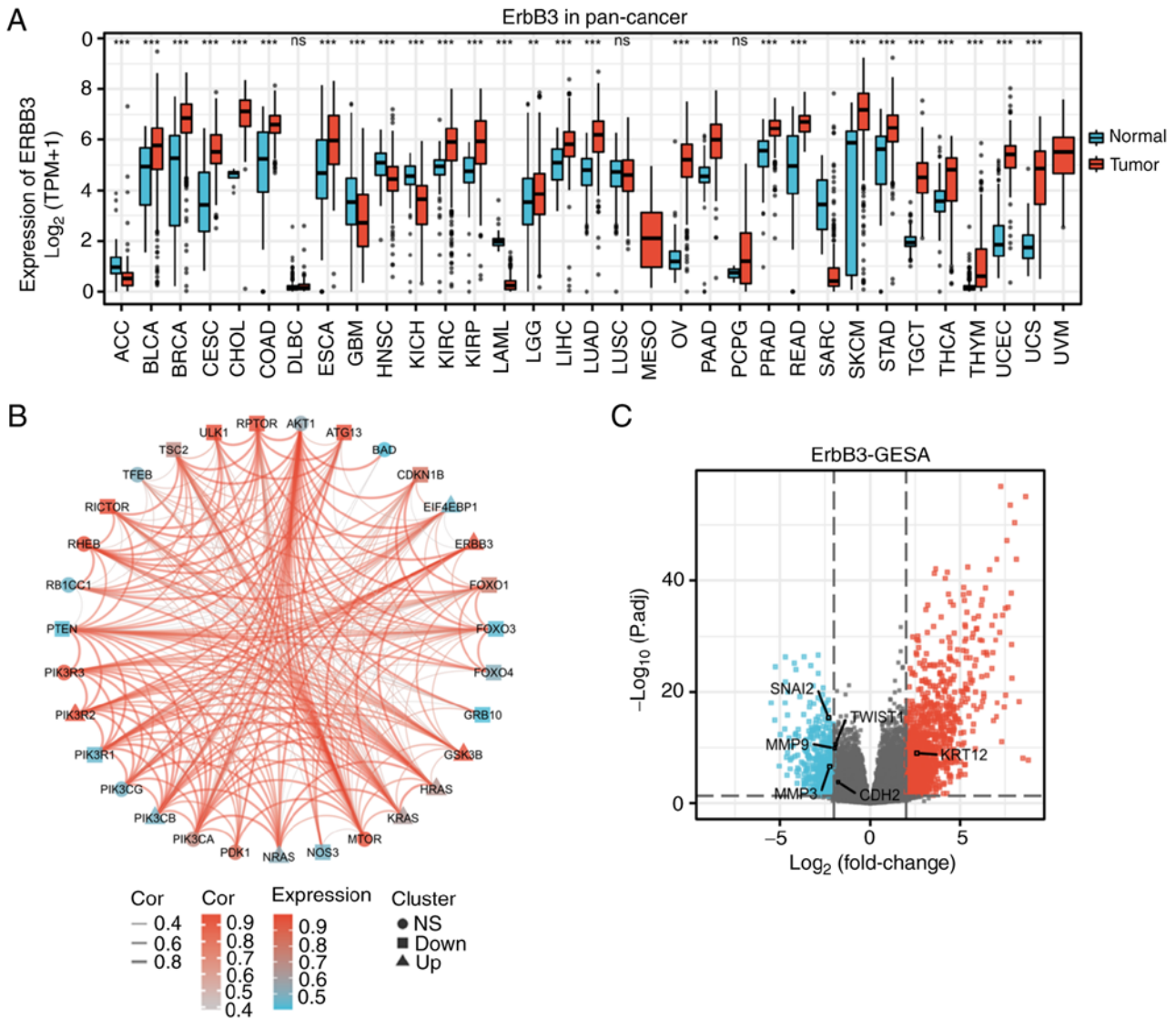
Figure 1. ERBB3 multiomic analysis. (A) RNA-seq TPM of tumor tissue and normal tissue in in different types of cancer to demonstrate ERBB3 (ENSG00000065361) expression (Wilcoxon rank-sum test; ns, not significant; **P<0.01; ***P<0.001). (B) Circle-curve correlation diagram of the ERBB3 and 30 genes related to the PI3K/AKT/mTOR pathway in CESC. The upright triangles represent the highly expressed genes, the inverted triangles represent the poorly expressed genes and the circles represent genes that have no significantly different expression in cervical cancer. (C) Volcano map of differentially-expressed genes, where red represents the upregulated genes and light blue represents the downregulated genes. Seq, sequencing; ERBB3; TPM, transcripts per million reads; ns, not significant; CESC, cervical squamous cell carcinoma and adenocarcinoma.

stack. The function of genes was divided into three categories: BPs, CCs and MFs.

Significant differences in EMT-related gene expression in cervical cancer were revealed. The following gene expression levels were upregulated: E-cadherin (CDH1), VIM, TWIST1, MMP3 and MMP9. The following gene expression levels were downregulated: N-cadherin (CDH2), SNAI2, MMP2, zinc finger E-box-binding homeobox 1 (ZEB1), integrin-linked protein kinase (ILK), RHO, TJP1 and SNAIL1 (Fig. 7). Further study on the correlation degree of ERBB3- and EMT-related factors revealed the following results: R=0.307, P<0.001 for KRT12; R=0.323, P<0.001 for TJP1; R=-0.407, P<0.001 for TWSIT1; and R=-0.306, P<0.001 for MMP9 (Fig. 8).

*Transcriptomics.* The key regulators in the PI3K/AKT/mTOR pathway are as follows: AKT1, BAD, CDKN1B, FOXO1, FOXO3, FOXO4, GSK3B, HRAS, KRAS, NOS3, NRAS, PDK1, PIK3CA, PIK3R3, PTEN, RPTOR, TSC2 and ULK1. It was revealed that nine transcription factors (TSC22D3, TP53, AR, RELA, NFKB1, STAT3, PPARG, SP1 and JUN) were associated with the regulation of the PI3K/AKT/mTOR pathway (Table I).

*Proteomics.* By comparing with the RNA level in normal cervical epithelium (Fig. 9A), it was revealed that the expression level of MMP9 in cervical cancer was significantly different. Through IHC analysis of the mRNA-protein expression of the EMT-related genes in cervical cancer tissues, it was revealed that the expression level of MMP family was relatively higher compared with those of other EMT-related genes (Fig. 9B). EMT of cervical cancer is associated with upregulation of MMP9. According to our previous findings of ERBB3 sequencing of cervical cancer cell lines (43), the mRNA levels of different primary cervical cancer cell lines indicated that
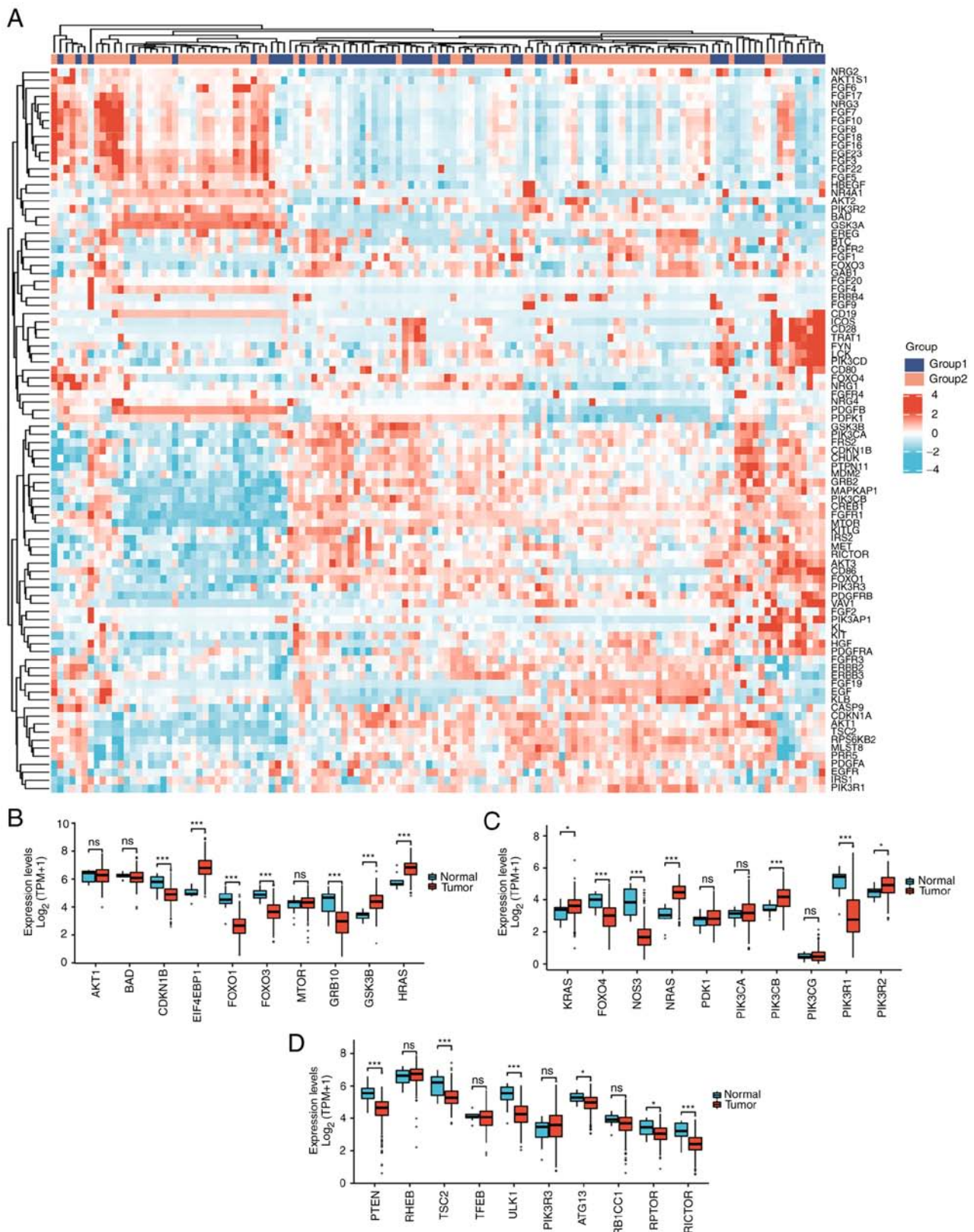
Figure 2. (A) Heat map of the expression levels of 89 PI3K/AKT signaling-related genes in CESC differentially-expressed genes (group 1 as the reference group for GSE63514 and GSE9750, and group 2 as the test group for GSE44001). (B) Differential gene expression between tumor and normal tissues for 10 genes in the PI3K/AKT/mTOR signaling pathway. (C) Differential gene expression between tumor and normal tissues for 10 genes in the PI3K/AKT/mTOR signaling pathway. (D) Differential gene expression between tumor and normal tissues for 10 genes in the PI3K/AKT/mTOR signaling pathway. *P<0.05 and ***P<0.001. ns, not significant; CESC, cervical squamous cell carcinoma and adenocarcinoma. For visualization purposes, (B-D) display a total of 30 genes in the PI3K/AKT/mTOR signaling pathway.

ERBB3 is highly expressed in cervical malignant cell lines dominated by SiHa and HeLa (Fig 9C). After further research
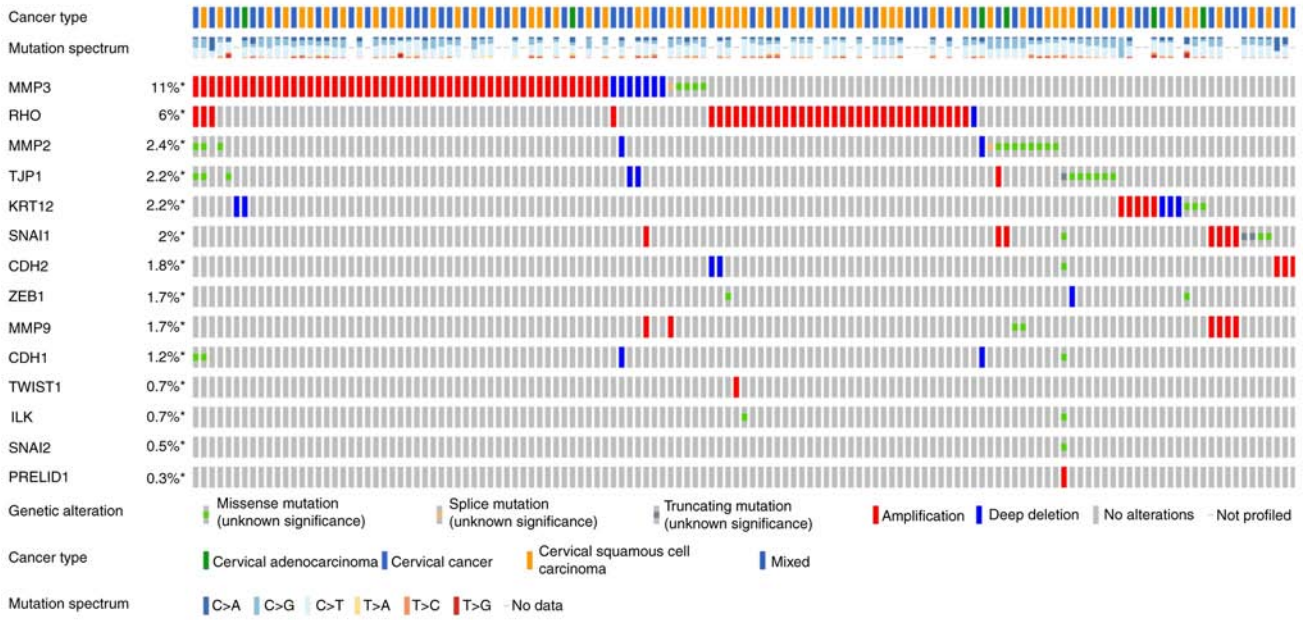
Figure 3. Genomic alteration types and alteration frequency of 14 EMT-associated genes in CESC were analyzed through the 'OncoPrint' module and 'Cancer Types Summary' module. CDH1, E-cadherin; KRT12, cytokeratin 12; TJP1, tight junction protein 1; CDH2, N-cadherin; VIM, vimentin; ZEB1, zinc finger E-box-binding homeobox 1; ILK, integrin-linked protein kinase.
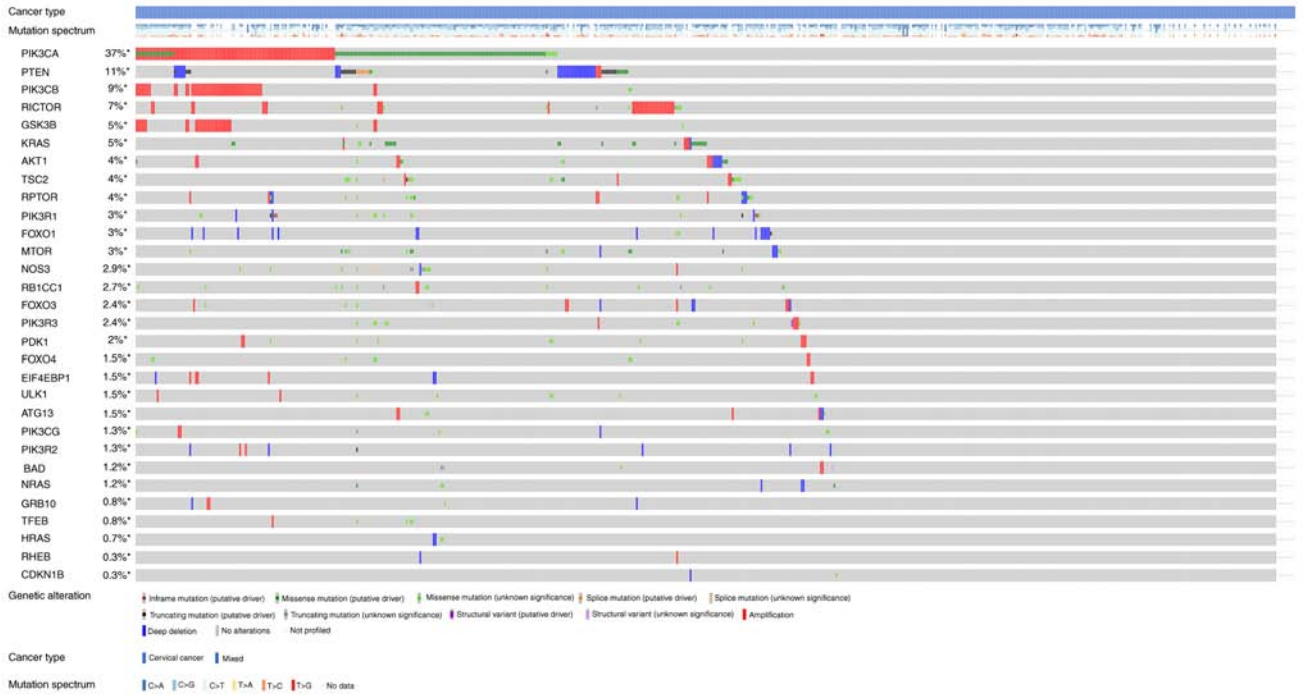


Figure 4. Genomic alteration types and alteration frequency of 30 PI3K/AKT/mTOR pathway-associated genes in CESC were analyzed through the 'OncoPrint' module and 'Cancer Types Summary' module.

on pathological types and HPV typing, it was revealed that in the three types of cells with higher expression of ERBB3, there was no significant difference between SiHa and HeLa, while there was a significant difference between SiHa and C33A (P<0.0001). These data show that ERBB3 is closely associated with adenocarcinoma and HPV-positive cervical carcinoma. Fig. 10 shows the protein interactions of the 30 key factors in the PI3K/AKT/mTOR signaling pathway with ERBB3. The

color of the lines in the figure shows that ERBB3 may play a stimulating role in the PI3K/AKT/mTOR pathway.

*EMT status and immuno-oncology insights from the RNA-seq-based analyses*
*Immune microenvironment characteristics of CESC.* ERBB3 influenced the survival time of patients with CESC, partially through immune cell infiltration. Enriched basophils (P<0.05),
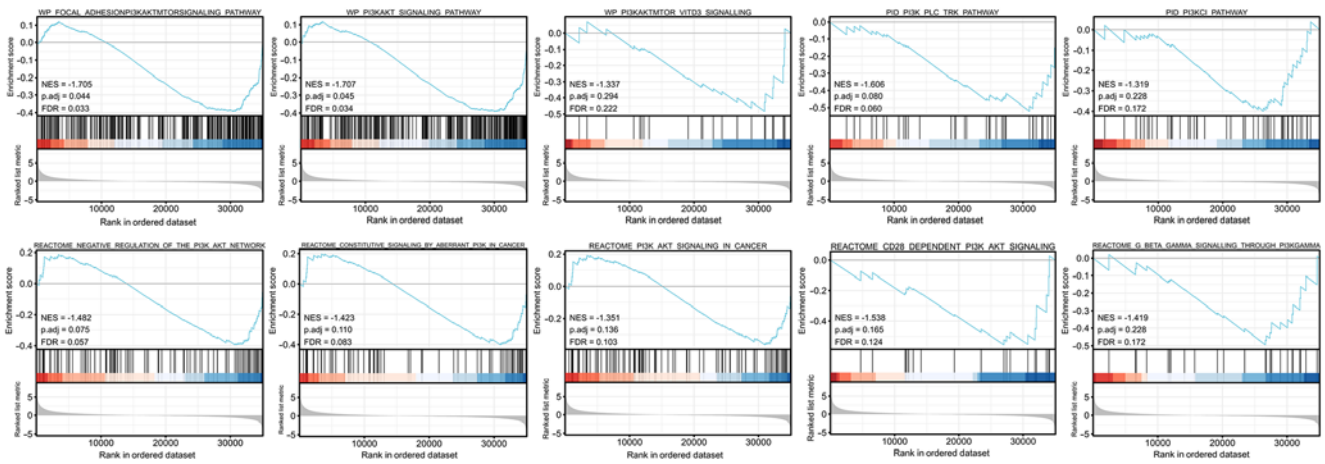
Figure 5. Gene set enrichment analysis of ERBB3. The present study considered that the threshold of significant enrichment was as follows: FDR <0.25, NES <0 and P<0.05. FDR, false-discovery rate; NES, normalized enrichment score.
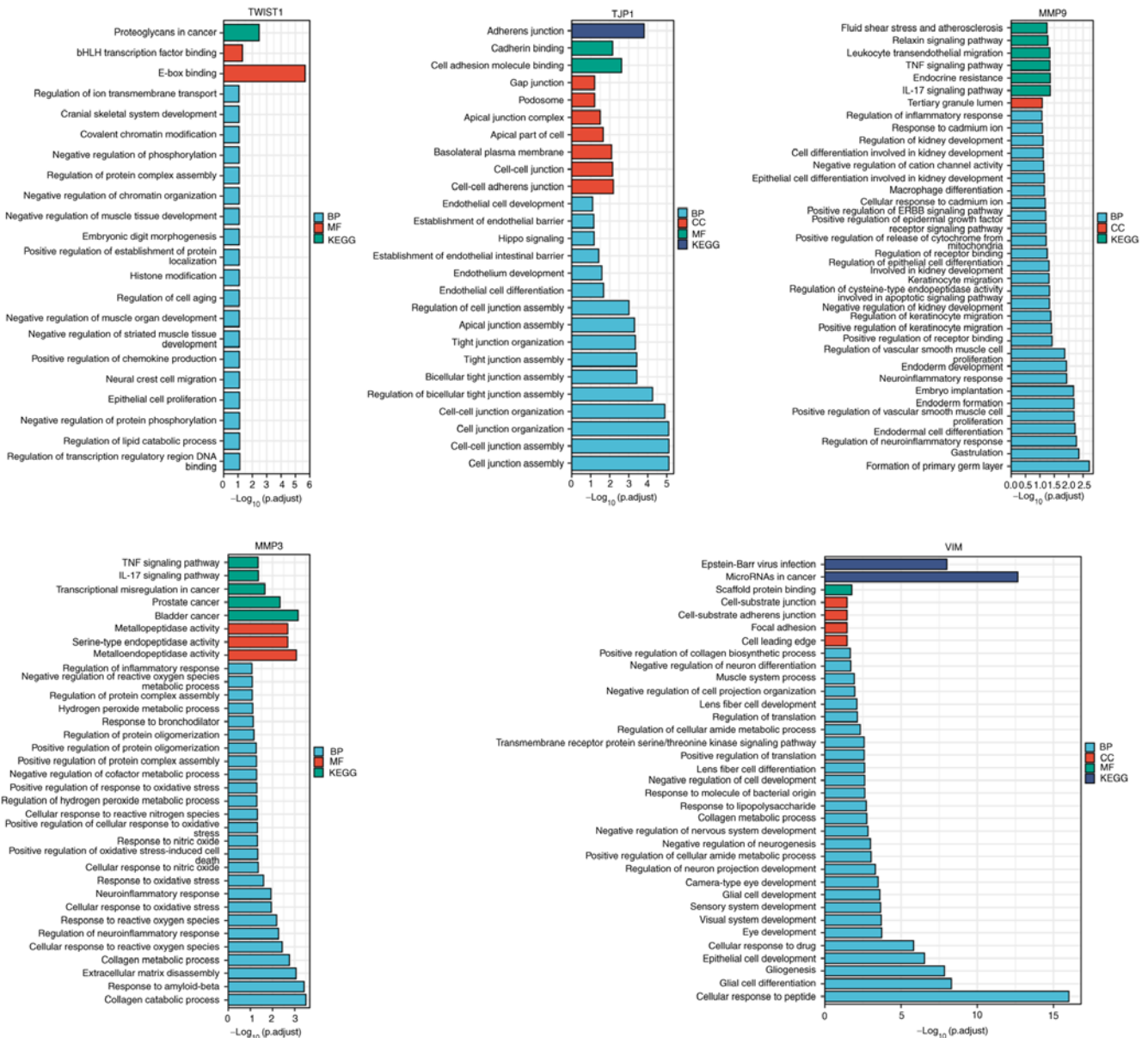


Figure 6. GO-KEGG cluster analysis. The x-axis represents '-log(adj. P)'; the greater the value, the stronger the significance. The y-axis represents the GO term. Each color represents an enrichment, including BP, CC, MF and KEGG. KEGG, Kyoto Encyclopedia of Genes and Genomes; GO, Gene Ontology; BP, biological processes; CC, cellular components; MF, molecular functions; TJP1, tight junction protein 1; VIM, vimentin.
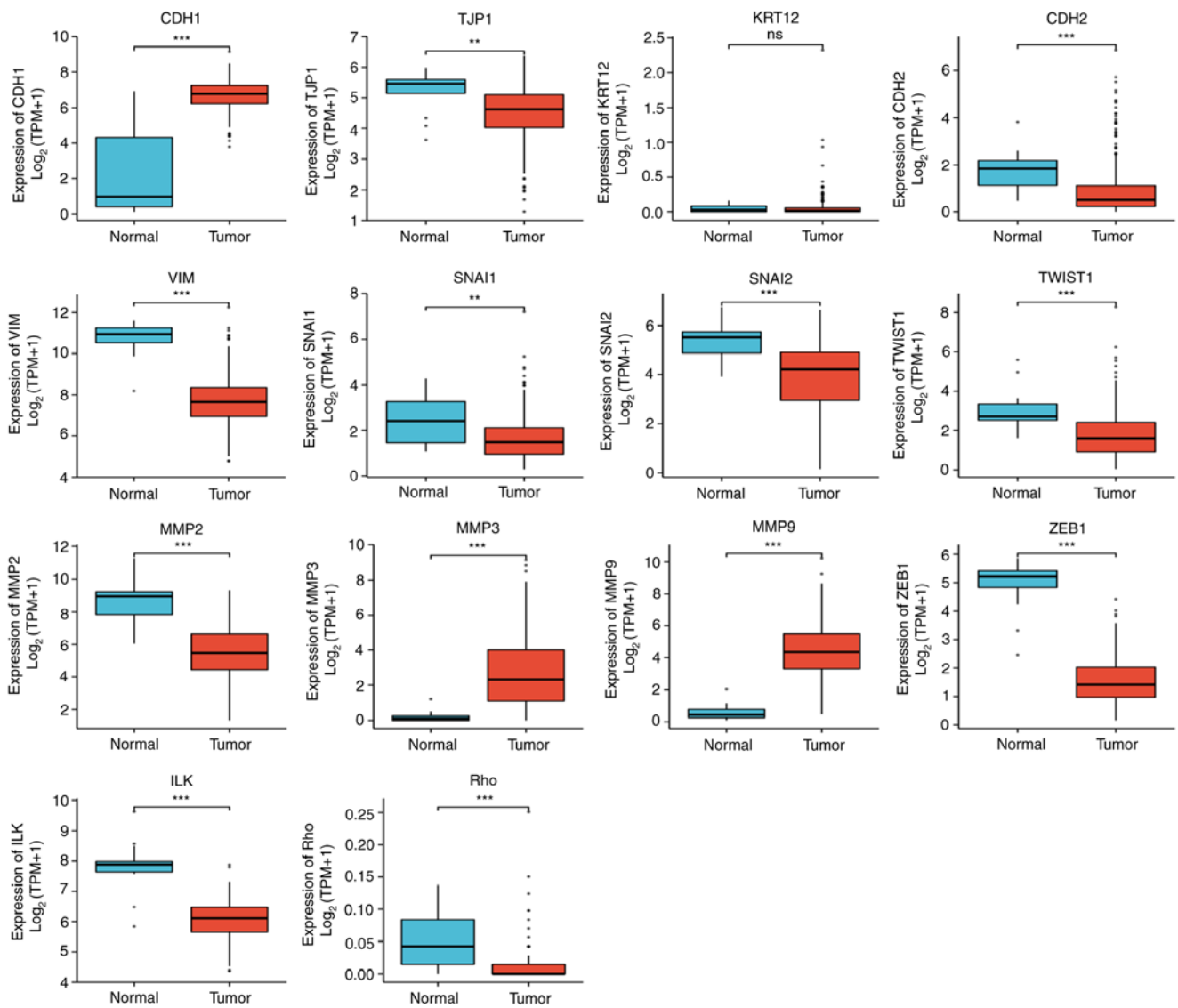
Figure 7. The following significant differences in the expression of epithelial-mesenchymal transition related-factors in CESC were found: CDH1↑, CDH2↓, VIM↑, SNAI2↓, TWIST1↑, MMP2↓, MMP3↑, MMP9↑, ZEB1↓, ILK↓, RHO↓, TJP1↓ and Snail1↓ (statistical method, Wilcoxon rank-sum test). **P<0.01 and ***P<0.001. Ns, not significant; CDH1, E-cadherin; KRT12, cytokeratin 12; TJP1, tight junction protein 1; CDH2, N-cadherin; VIM, vimentin; ZEB1, zinc finger E-box-binding homeobox 1; ILK, integrin-linked protein kinase.

decreased B cells (P<0.05), enriched CD4+ memory T cells (P<0.05), enriched mesenchymal stem cells (P<0.05), decreased eosinophils (P<0.05), decreased natural-killer T cells (P<0.05), decreased CD8+ memory T cells (P<0.01) and decreased macrophages (P<0.01). Among the abovementioned eight types of immune cell infiltration, the prognosis of the group with a higher ERBB3 mRNA level was decreased (Fig. 11).

*EMT-related genes change the immune cell infiltration.* If the absolute value of R is below 0.3, there is no straight phase off; R of ≥0.3 denotes linear correlations; R values between 0.3 and 0.5 indicate low-degree correlations; R values between 0.5 and 0.8 refer to significant correlations; and R values of 0.8 and above are high-degree correlations. As shown in Table II, correlation between the EMT-related factors and immune cell infiltration was not high. Among the EMT-related factors, MMP9, MMP2, and ZEB1 were

closely associated with the immune system. The EMT status (Fig. 12) may be related to MMP9 changing the tumor immune microenvironment through dendritic cells and macrophages (10).

*Prognostic analysis of microenvironment phenotypes.* Statistically significant EMT-related genes that can predict the OS index of CESC included KRT12 (P<0.05), VIM (P<0.05), SNAI1 (P<0.05), ILK (P<0.05), CDH2 (P<0.01), MMP2 (P<0.01) and MMP3 (P<0.01). All of the seven factors were the risk factors for CESC (Fig. 13).

Risk score was constructed using eight selected genes through the multifactor analysis of the disease prognosis model, and three prognostic types of OS, disease-specific survival and progression-free interval (PFI) were analyzed. ERBB3, CD47, MMP9, TWIST1, CDH2, PTEN, VIM and ZEB1 were included. Multivariate analysis revealed that CDH2, MMP9, and VIM were significant factors in the
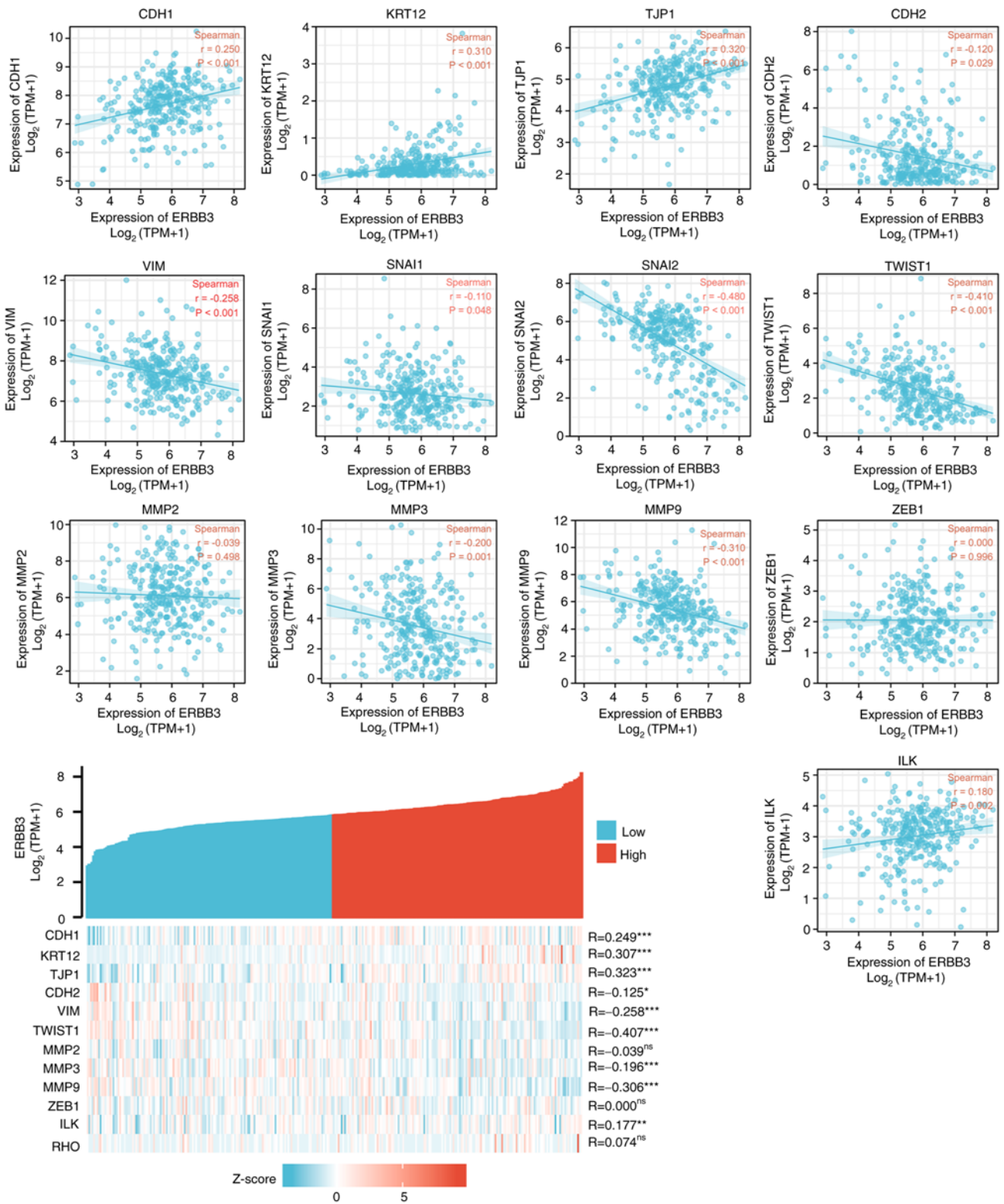
Figure 8. Correlation between ERBB3 and factors associated with epithelial-mesenchymal transition status. Statistically significant were TWIST1 (R=-0.407; P<0.001), TJP1 (R=0.323; P<0.001), KRT12 (R=0.307; P<0.001), MMP9 (R=-0.306; P<0.001). Statistical method, Spearman's correlation; *P<0.05, **P<0.01 and ***P<0.001. ns, not significant; CDH1, E-cadherin; KRT12, cytokeratin 12; TJP1, tight junction protein 1; CDH2, N-cadherin; VIM, vimentin; ZEB1, zinc finger E-box-binding homeobox 1; ILK, integrin-linked protein kinase.

assessment of PFI. Gene signatures of cervical cancer cell immune-oncology microenvironment positively correlated with the patients' survival. These analyses (Fig. 14) indicated that the selected genes and constructed risk prognostic models had good prognostic value.

## Discussion

High-risk HPV16 DNA is integrated into the host cell genome (HPV16: q21-q31 of chromosome 2.13; HPV18: chromosome 24.8) (44), disrupts the open reading frame, and

Table I. Key transcription factors of PI3K/AKT/mTOR biomarkers in cervical squamous cell carcinoma and adenocarcinoma.

| Key transcription factor | Description | Regulated gene | P-value | FDR |
|---|---|---|---|---|
| TSC22D3 | TSC22 domain family, member 3 | FOXO4, FOXO3, FOXO1 | $3.62 \times 10^{-8}$ | $3.26 \times 10^{-7}$ |
| TP53 | Tumor protein p53 | HRAS, PTEN, CDKN1B, AKT1, FOXO3 | $5.57 \times 10^{-6}$ | $2.51 \times 10^{-5}$ |
| AR | Androgen receptor | AKT1, TSC2, NRAS, PTEN | $1.37 \times 10^{-5}$ | $4.12 \times 10^{-5}$ |
| RELA | V-rel reticuloendotheliosis viral oncogene homolog A (avian) | PTEN, BAD, FOXO3, NOS3, AKT1 | $1.02 \times 10^{-4}$ | $1.90 \times 10^{-4}$ |
| NFKB1 | Nuclear factor of kappa light polypeptide gene enhancer in B-cells 1 | PTEN, AKT1, GSK3B, FOXO3, NOS3 | $1.06 \times 10^{-4}$ | $1.90 \times 10^{-4}$ |
| STAT3 | Signal transducer and activator of transcription 3 (acute-phase response factor) | PTEN, CDKN1B, AKT1 | $1.46 \times 10^{-3}$ | $2.19 \times 10^{-3}$ |
| PPARG | Peroxisome proliferator-activated receptor gamma | BAD, PTEN | $4.92 \times 10^{-3}$ | $6.33 \times 10^{-3}$ |
| SP1 | Sp1 transcription factor | CDKN1B, PTEN, NOS3, HRAS | $6.32 \times 10^{-3}$ | $7.11 \times 10^{-3}$ |
| JUN | Jun proto-oncogene | PDK1, NOS3 | $2.33 \times 10^{-2}$ | $2.33 \times 10^{-2}$ |

FOXO, Forkhead box; CDKN1B, cyclin-dependent kinase inhibitor 1B; TSC2, tuberous sclerosis 2; BAD, Bcl2-associated agonist of cell death; NOS3, nitric oxide synthase 3; GSK3B, Glycogen synthase kinase-3 β; PDK1, pyruvate dehydrogenase (acetyl-transferring) kinase isozyme 1.

causes overexpression of E6 and E7 genes (45). It has been demonstrated that E6 and E7 exert carcinogenic effects by combining with cell cycle regulators, such as p53 (a transcription factor related to the PI3K pathway as shown in Table I) and retinoblastoma (46). E6 can interact with E6-related protein E6AP to form a complex and bind to p53 (47), hydrolyze p53, and cause the loss of negative regulation of cell proliferation induced by p53, thereby leading to uncontrolled cell proliferation and malignant transformation. The present study also revealed that ERBB3 was highly expressed in HPV-infected cell lines and was associated with adenocarcinoma. Therefore, it can be speculated that HPV-positive cervical cancer cells and adenocarcinoma are the carcinogenic factors or prognostic factors of cervical cancer.

To investigate the association between the actual activation of the PI3K pathway and immune infiltration, the DEGs of ERBB3 in CESC was assessed (GSE63514, GSE9750 and GSE44001 datasets from the Gene Expression Omnibus database were analyzed) for hub genes of the PI3K/AKT/mTOR pathway and cancer progression. Pathway enrichment, protein-protein interaction and pathway crosstalk analyses were performed to identify key genes and pathways. The current study illustrated that cancer-immune interactions might differ depending on specific alterations in the PI3K pathway, demonstrating that genetic aberrations in malignant cells influence the immune landscape of tumors.

The diversity of EMT creates a wide range of heterogeneity in tumors, and may provide tumor cells with increased adaptability and resistance, enabling them to survive and proliferate in a complex TME, and metastasize and invade lymph and blood vessels. The present study demonstrated that MMPs, especially MMP9 as a prominent representative, are highly

relevant for TME and immune cells. MMPs are a family of zinc-dependent endopeptidases (48,49). The biological function of MMPs is to degrade various molecules used for cell adhesion and regulate the interaction between cells and the extracellular matrix. Recent studies (50-52) have shown that MMPs are highly associated with the microenvironment of tumors and immune cells, and targeting MMPs may overcome the barriers of immunosuppression. However, the present study revealed that the expression of MMP9 was not a significant predictor of OS in patients with cervical cancer. MMP9 was significantly associated with ERBB3.

In the complex TME, the same anti-infection immune cells can be destroyed by tumor cells (53). As a result, the antitumor immune cells not only do not destroy the transformed cells, but they even change to immune cells that promote tumor growth and metastasis (54,55). These immune cells secrete factors that promote survival, promote migration, and resist detection. Hence, the present study discussed the mechanism of accelerating cervical cancer tumor progression from the perspective of EMT-associated immune evasion.

Cellular immunity is necessary for clearing HPV-infected and HPV-transformed tumor cells. HPV-specific CD8 cytotoxic T lymphocytes (CTLs) are needed for the immune defense against cervical cancer. However, the function of CTLs may be blunted by systemic and local immunosuppressive environments associated with tumor growth (56,57). A series of clinical trials (58-60) have shown that the immune system is unable to completely eradicate the tumor despite the presence of HPV-specific T cells in HPV-associated neoplastic tissue, which suggests the possible existence of systemic immunosuppression and an immunosuppressive TME that significantly influence the efficacy of therapeutic vaccines.
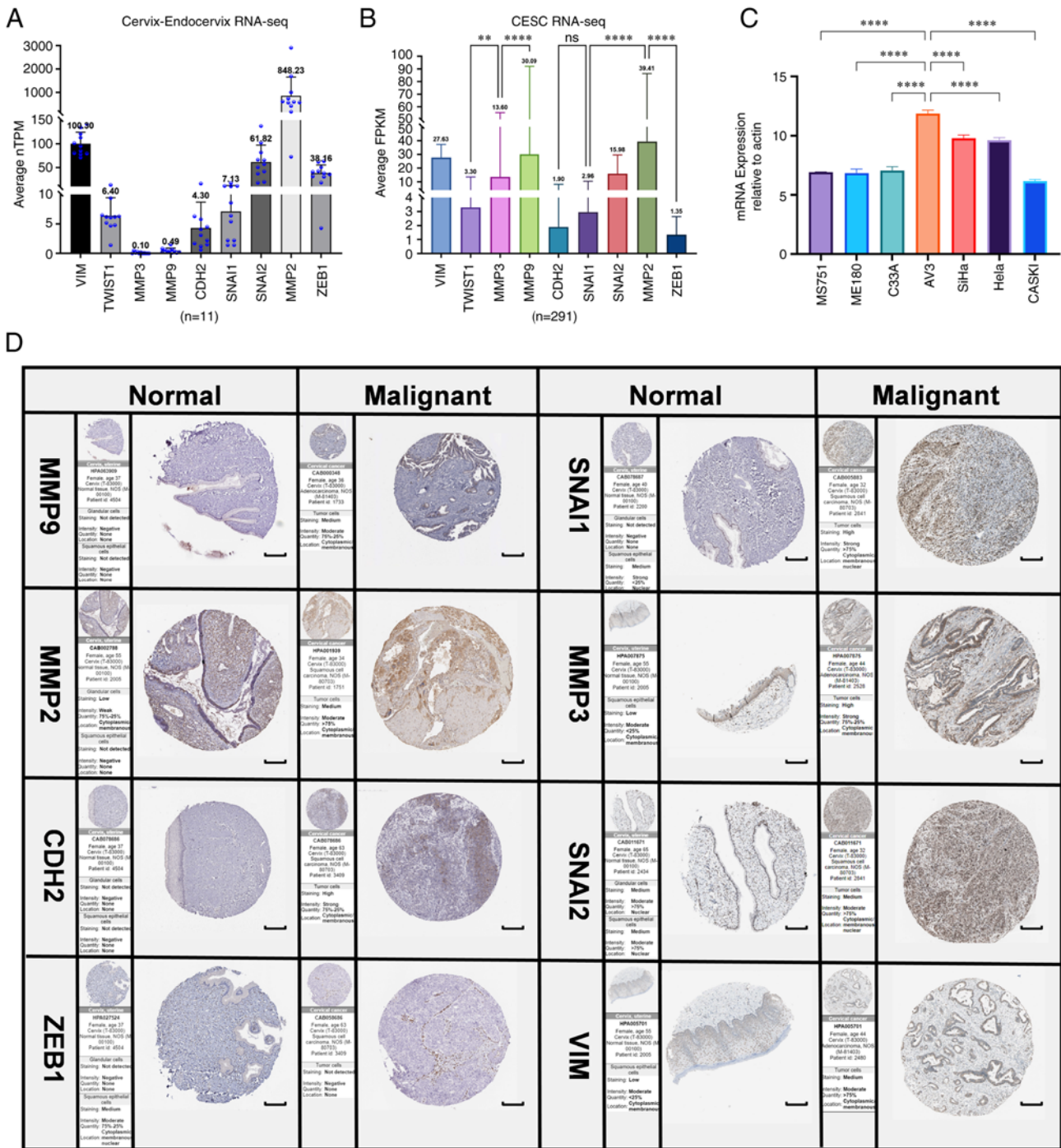
Figure 9. RNA-sequencing and protein level analysis of EMT upregulated factors (PRELI domain-containing protein 1, CDH2, TWIST1, MMP2, MMP3, MMP9, SNAI1, SNAI2 and ZEB1) in normal cervical epithelium and tumor tissues by immunohistochemistry for cervical cancer invasiveness assessment. (A) Normalized TPM was quantified, as shown. The dot plot depicts the means and standard deviation of 11 images of normal cervix-endocervix tissues. (B) FPKM was quantified of 291 images of cervical cancer tissues. (C) ERBB3 expression in seven different cell lines were examined using reverse transcription-quantitative PCR. All PCR data were calculated relative to β-actin and represent the average ± SD of triplicate samples. (D) Immunohistochemical validation of the most significant EMT-related genes in cervical cancer and normal cervix tissues by The Human Protein Atlas database (scale bars, 200 $\mu$m). The translational expression level (mRNA and protein) of the eight EMT-related genes was positively correlated with disease status as they were upregulated in cervical squamous cell carcinoma and adenocarcinoma samples. ANOVA followed by Tukey's multiple-comparison tests; **$P<0.01$ and ****$P<0.0001$. EMT, epithelial-mesenchymal transition; CDH1, E-cadherin; KRT12, cytokeratin 12; TJP1, tight junction protein 1; CDH2, N-cadherin; VIM, vimentin; ZEB1, zinc finger E-box-binding homeobox 1; ILK, integrin-linked protein kinase; FPKM, fragments per kilobase per million; ERBB3, Erb-B2 receptor tyrosine kinase 3; TPM, transcripts per million.

Tumor-associated macrophages (TAMs) may cause the disruptive change of antitumor immunity in TME and promote tumor growth and metastasis (61). TAMs are a heterogeneous population of cells that display a range of phenotypes depending on the type of tumor and their location in TME (62,63). TAMs are commonly the most abundant infiltrating leukocytes in most tumors and are predominantly thought to have pro-tumor effects. These include both immunosuppressive effects in
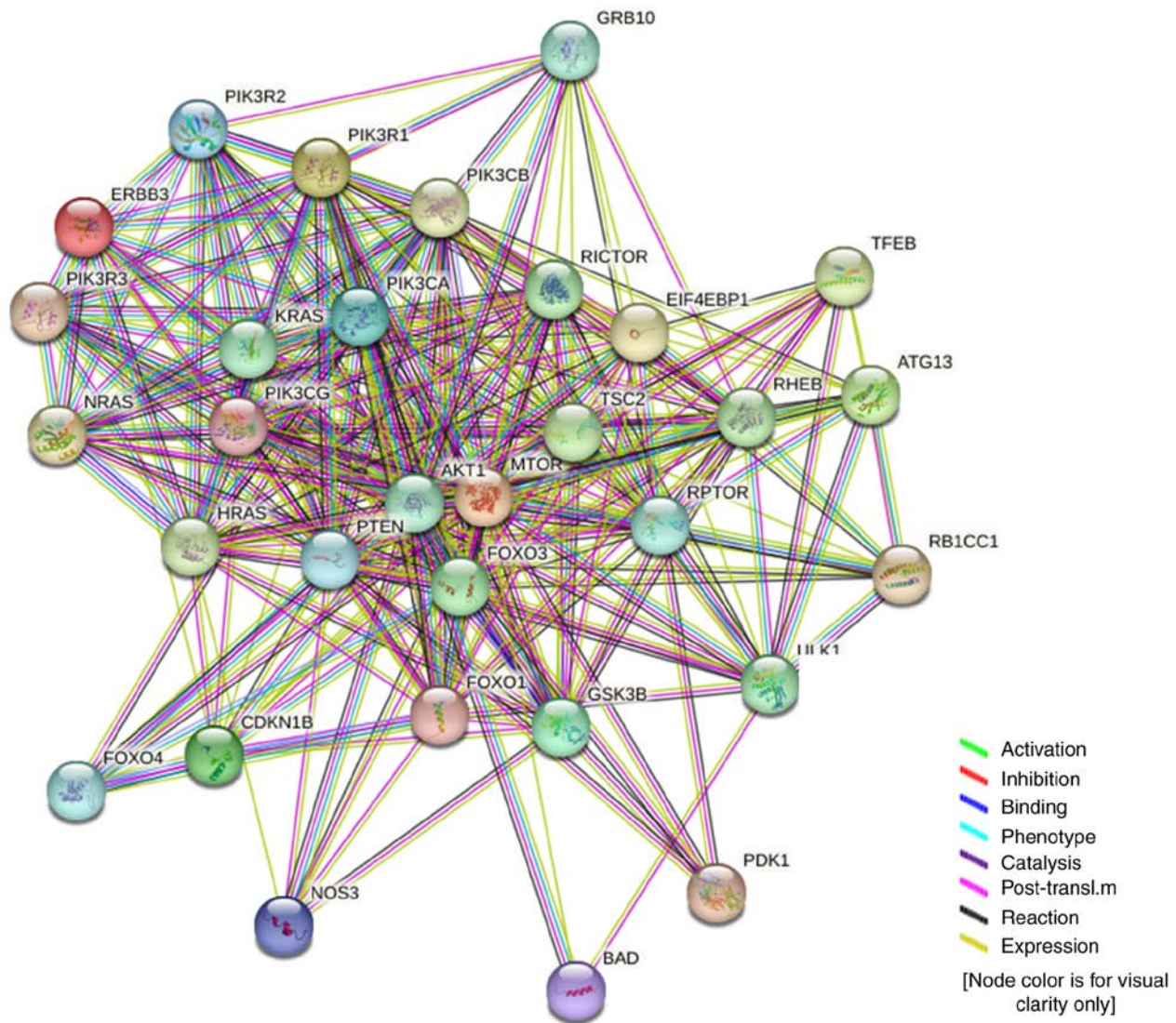
Figure 10. STRING interaction network in the PI3K/AKT/mTOR signaling pathway to show the protein-protein interaction with ERBB3.

addition to pro-antigenic and metastatic effects. TAMs also promote tumor immune evasion through expression of signal regulatory protein α (SIRPα) (64,65). SIRPα is a receptor for CD47 (66), a cell surface protein that typically protects normal cells from phagocytosis by macrophages or dendritic cells. CD47 is frequently overexpressed on tumor cells and plays a key role in tumor escape by binding to SIRPα and sending macrophages a 'don't eat me' signal (67,68). Blockade of the CD47-SIRPα signal has been shown to stimulate phagocytosis, leading to tumor cell elimination (69).

In the present study, TAMs were revealed to drive tumor angiogenesis and progression in a spontaneous model of cervical cancer through the production of MMP-9. Previous studies (60,70) showed that MMP9 alone did not significantly affect the survival rate of cervical cancer; however, in the present study, when TME macrophages decreased, there was an impact on OS, and the OS with high ERBB3 was significantly reduced. The GO and KEGG enrichment of MMP9 demonstrated that it participated in the biological process of the IL-17 signaling pathway. In patients with bullous pemphigoid, monocyte-derived macrophages, but not lymphocytes,

respond to CXCL10 (upregulated by IL-17) by increasing MMP-9 release, potentially creating an inflammatory loop associated with disease outcome (71).

Late after pattern recognition receptors stimulation, bone-marrow-derived dendritic cells (BMDCs) induce the glucose transporter GLUT1 (72,73) and commit to aerobic glycolysis via the mTOR-HIF-1α/iNOS axis (74), which generates NO, inhibiting the electron transport chain. This process might decrease expression of MHC and co-stimulatory molecules by activated BMDCs (75).

Intratumoral immune cells are more often present in tumors with increasing PI3K downstream phosphorylation (76-78). This is most pronounced for MMP9-positive cells. Research data shows that disturbances in the PI3K pathway may help immune escape (79). A prospective trial in cervical cancer suggested that PI3K pathway alterations may be associated with the composition of TME (80,81).

Previous studies (82-84) have suggested that when cells undergo EMT and shift progressively from an epithelial to a mesenchymal state, genetic alterations include decreased expression levels of CDH1, cytokeratin 12 and TJP1, increased
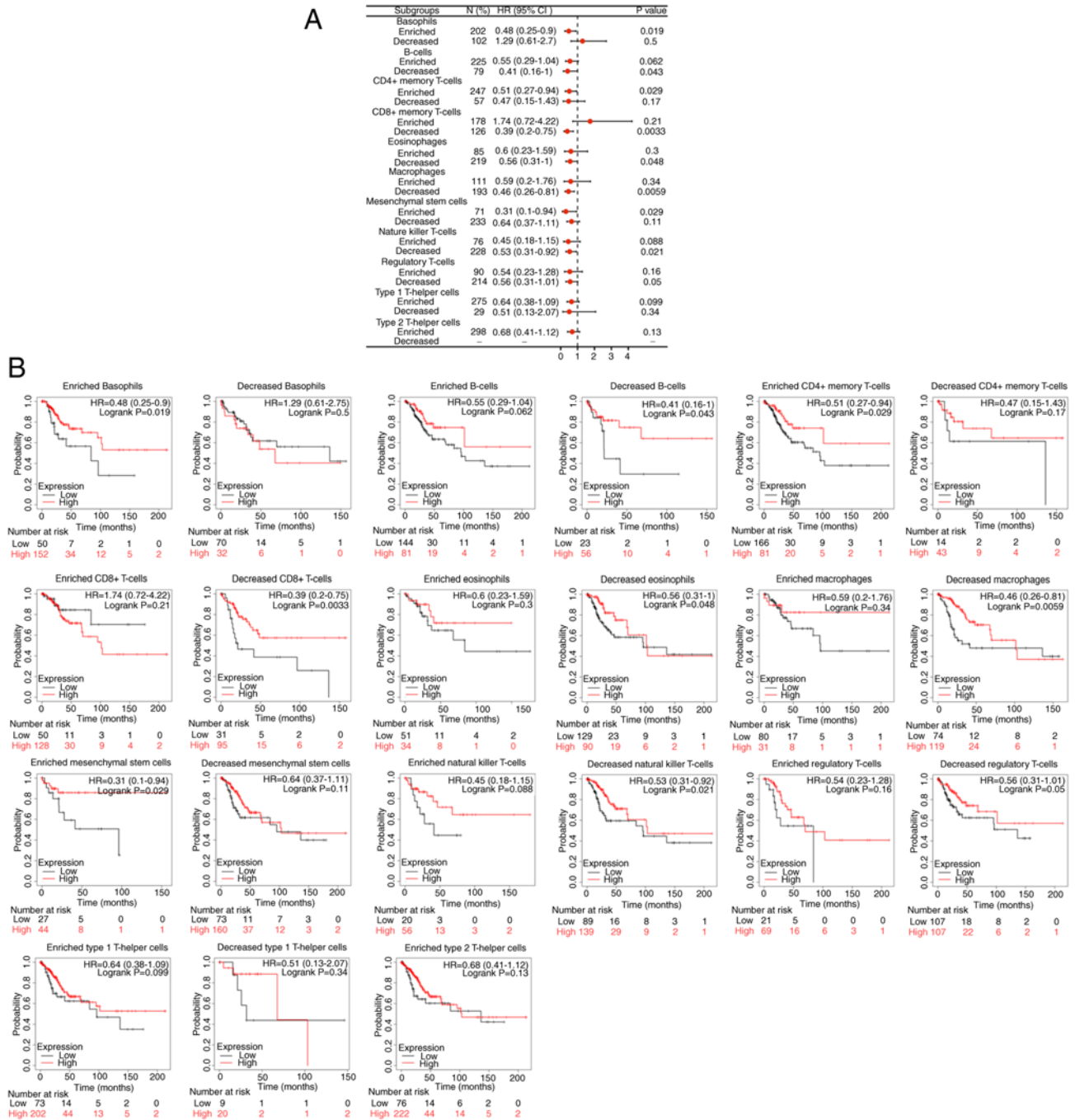
Figure 11. Kaplan-Meier survival curves according to high and low expression of ERBB3 in immune cell subgroups in CESC. (A) A forest plot shows the six prognostic values of ERBB3 expression according to different immune cell subgroups in patients with CESC. (B) Associations between ERBB3 expression and overall survival in different immune cell subgroups in patients with CESC were estimated using Kaplan-Meier plotter. CESC, cervical squamous cell carcinoma and adenocarcinoma samples; HR, hazard ratios.

expression levels of CDH2, VIM, SNAI1, SNAI2, TWIST1, MMP2, MMP3, MMP-9 and ZEB1 and increased activity of ILK and RHO.

It can be inferred from the present study that tumor infiltration by CD8-positive lymphocytes was associated with PIK3CA mutations and worse clinical outcome. At the molecular level, EMT transcriptional factors, including SNAl, ZEB1 and TWIST1, regulated immunosuppressive cells or enhanced the expression of immunosuppressive checkpoint molecules through the production of chemokines, thereby resulting in immunosuppression of TME. Immunosuppressive

factors can also induce EMT in tumor cells. This mutual feedback between EMT and immunosuppression promotes tumor progression (85).

In conclusion, integrating the characteristics of biomarkers in multiple dimensions can ensure the most efficient management choice for each patient with cancer (Fig. 15). The EMT status cannot be assessed based on one or a few molecular markers, but should be assessed in conjunction with changes in cell characteristics to assess the current ability of cell metastasis and distant invasion. Immuno-oncology research can generate the discriminating power and richness of data

Table II. ERBB3 methylation and immune infiltration in tumor microenvironment of cervical cancer.

| Cell type | CDH1 | CDH2 | ERBB3 | ILK | KRT12 | MMP2 | MMP3 | MMP9 | PRELID1 | RHO | SNAI2 | SNAI1 | TJP1 | TWIST1 | ZEB1 |
|---|---|---|---|---|---|---|---|---|---|---|---|---|---|---|---|
| aDC | -0.172[a] | -0.173[a] | -0.283[b] | -0.132 | -0.041 | -0.038 | 0.124[c] | 0.427[b,d] | 0.028 | -0.051 | 0.183[a] | 0.033 | -0.159[a] | 0.015 | 0.046 |
| B cells | -0.131[c] | -0.074 | -0.078 | -0.134 | -0.085 | 0.127[c] | -0.016 | 0.293[b] | 0.014 | -0.000 | -0.072 | -0.004 | -0.128[c] | -0.005 | 0.217[b] |
| CD8 T cells | -0.222[c] | 0.042 | -0.137[c] | -0.067 | -0.031 | 0.069 | 0.022 | 0.228[b] | 0.056 | 0.072 | -0.099 | 0.159[a] | -0.129[c] | 0.090 | 0.247[b] |
| Cytotoxic cells | -0.318[c,d] | -0.130[c] | -0.177[a] | -0.219[b] | -0.068 | -0.021 | 0.040 | 0.306[b,d] | 0.077 | 0.003 | 0.031 | 0.049 | -0.231[b] | -0.017 | 0.054 |
| DC | -0.081 | -0.005 | -0.095 | -0.099 | 0.030 | 0.182[a] | 0.184[a] | 0.527[c,e] | 0.064 | -0.094 | 0.065 | 0.121[c] | -0.097 | 0.011 | 0.131[c] |
| Eosinophils | 0.037 | 0.285[b] | 0.052 | 0.165[a] | 0.103 | 0.339[b,d] | 0.084 | 0.184[a] | 0.009 | 0.157[a] | -0.078 | 0.316[b,d] | -0.022 | 0.202[b] | 0.404[b,d] |
| iDC | -0.165[a] | 0.092 | -0.226[b] | -0.045 | -0.094 | 0.334[b,d] | 0.048 | 0.505[b,e] | 0.006 | -0.019 | 0.233[b] | 0.095 | -0.092 | 0.160[a] | 0.283[b] |
| Macrophages | -0.048 | 0.301[b] | -0.313[b,d] | 0.021 | -0.073 | 0.449[b,d] | 0.266[b] | 0.526[c,e] | 0.142[c] | -0.005 | 0.210[b] | 0.393[b,d] | -0.067 | 0.281[b] | 0.376[b,d] |
| Mast cells | 0.025 | 0.328[b,d] | 0.062 | 0.066 | 0.126[c] | 0.485[b,d] | 0.214[b] | 0.177[a] | -0.108 | 0.109 | 0.011 | 0.219[b] | 0.084 | 0.234[b] | 0.466[b,d] |
| Neutrophils | -0.050 | 0.128[c] | -0.214[b] | 0.011 | 0.062 | 0.181[a] | 0.415[b,d] | 0.420[b,d] | 0.112 | -0.160[a] | 0.127[a] | 0.341[b] | 0.015 | 0.072 | 0.142[c] |
| NK CD56 bright cells | -0.123[a] | 0.136[c] | 0.312[b,d] | 0.012 | 0.193[b] | 0.013 | -0.019 | -0.111 | -0.081 | 0.140[c] | -0.463[b,d] | 0.089 | -0.061 | -0.131[c] | 0.014 |
| NK CD56dim cells | -0.208[b] | -0.122 | -0.261[b] | -0.174[a] | -0.076 | 0.004 | 0.149[a] | 0.370[c,d] | 0.028 | -0.089 | 0.208[b] | 0.108 | -0.167[a] | 0.012 | 0.039 |
| NK cells | -0.066 | 0.434[b,d] | -0.088 | 0.229[b] | -0.094 | 0.471[b,d] | 0.054 | 0.083 | 0.043 | 0.190[b] | -0.072 | 0.349[b] | -0.072 | 0.301[b] | 0.455[b,d] |
| pDC | -0.229[c] | 0.155[a] | -0.062 | -0.121 | -0.004 | 0.157[a] | -0.018 | 0.188[b] | 0.070 | 0.113[c] | -0.275[b] | 0.051 | -0.296[b] | 0.124[c] | 0.245[b] |
| T cells | -0.213[c] | -0.148[a] | -0.111 | -0.137 | -0.109 | 0.020 | -0.007 | 0.319[b,d] | 0.052[a] | 0.012 | -0.018 | 0.049 | -0.165[a] | -0.055 | 0.153[a] |
| T helper cells | 0.079 | -0.070 | -0.006 | 0.174[a] | -0.022 | 0.006 | -0.106 | 0.146[c] | -0.015 | 0.029 | 0.059 | 0.019 | 0.162[b] | -0.085 | 0.279[b] |
| TCM | 0.209[b] | -0.114[c] | -0.113[c] | 0.199[b] | -0.017 | 0.091 | -0.060 | 0.148[a] | -0.182 | -0.077 | 0.358[b,d] | -0.093 | 0.318[b,d] | 0.032 | 0.195[b] |
| TEM | 0.062 | 0.260[b] | 0.038 | 0.224[b] | -0.014 | 0.307[b,d] | 0.075 | 0.157[a] | 0.101 | 0.078 | -0.273[b] | 0.269[b] | -0.064 | 0.095 | 0.391[b,d] |
| TFH | -0.061 | 0.116[c] | -0.124[c] | 0.007 | -0.113[c] | 0.262[b] | 0.017 | 0.246[b] | 0.032 | 0.128[c] | -0.088 | 0.194[b] | -0.118[c] | 0.172[a] | 0.396[b,d] |
| TGD | -0.079 | -0.057 | -0.239[b] | -0.025 | -0.013 | 0.007 | 0.280[b] | 0.219[b] | -0.011 | -0.061 | 0.292[b] | 0.055 | 0.028 | 0.057 | -0.010 |
| Th1 cells | -0.211[b] | -0.030 | -0.374[b,d] | -0.136 | -0.082 | 0.133[c] | 0.265[b] | 0.468[b,d] | -0.014 | -0.098 | 0.263[b] | 0.202[b] | -0.160[a] | 0.157[a] | 0.127[c] |
| Th17 cells | -0.099 | -0.106 | 0.082 | -0.095 | -0.015 | -0.099 | 0.099 | 0.031 | 0.136[c] | 0.140[c] | -0.234[b] | 0.040 | -0.075 | -0.266[b] | -0.049 |
| Th2 cells | 0.118[c] | 0.067 | -0.140[c] | 0.235[a] | 0.014 | 0.170[a] | 0.183[a] | 0.162[a] | -0.043 | -0.007 | 0.240[b] | 0.130[c] | 0.083 | 0.218[b] | 0.239[b] |
| T Reg | -0.183[a] | -0.103 | -0.285[b] | -0.163[a] | -0.127[c] | 0.064 | 0.063 | 0.435 | 0.033 | -0.038 | 0.170[a] | 0.058 | -0.213[b] | 0.070 | 0.118[c] |

The significance of correlations between immune cell infiltration in cervical cancer tissue and the expression of different genes was determined using Spearman's rank correlation coefficient. [a]P<0.01, [b]P<0.001 and [c]P<0.05; [d]moderate and [e]high correlation. CDH, cadherin; ILK, integrin-linked protein kinase; KRT12, cytokeratin 12; PRELID1, PRELI domain-containing 1; TJP1, tight junction protein 1; ZEB1, zinc finger E-box-binding homeobox 1; DC, dendritic cells; NK, natural killer cells; Th, T helper; aDC, activated DC; iDC, immature DC; pDC, plasmacytoid DC; TCM, T central memory; TEM, T effector memory; TFH, T follicular helper; TGD, T γδ.
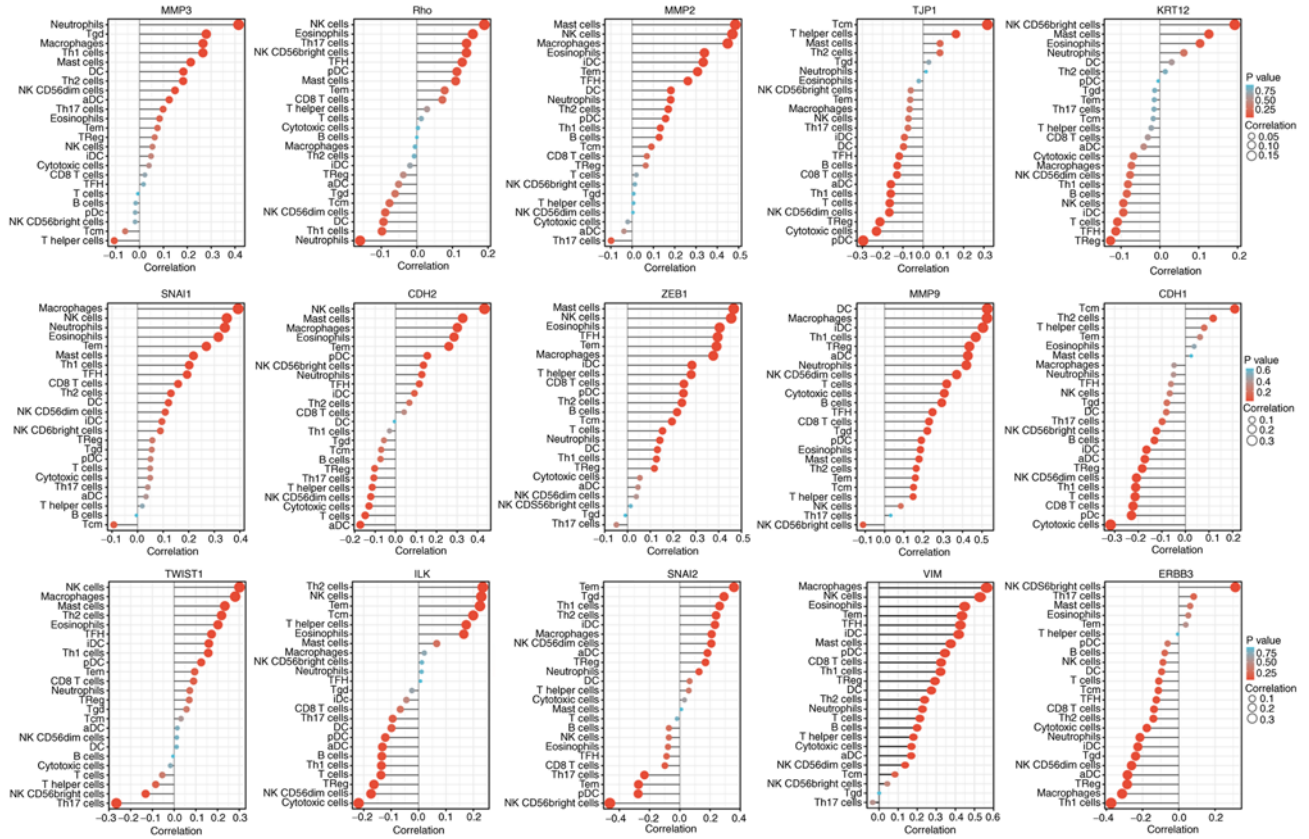
Figure 12. Single sample GSEA enrichment set the score to infer the infiltration by immune cells in each sample. The size of the circle represents the degree of relevance. The greater the height of the bar (the distance from 0), the higher the degree of correlation (a positive number represents a positive correlation, and a negative number represents a negative correlation). The depth of the circle represents the P-value obtained by the correlation analysis, the legend on the right is the color scale value, and the range of the color scale is automatically generated according to the range of the P-value obtained in the figure. CDH1, E-cadherin; KRT12, cytokeratin 12; TJP1, tight junction protein 1; CDH2, N-cadherin; VIM, vimentin; ZEB1, zinc finger E-box-binding homeobox 1; ILK, integrin-linked protein kinase.
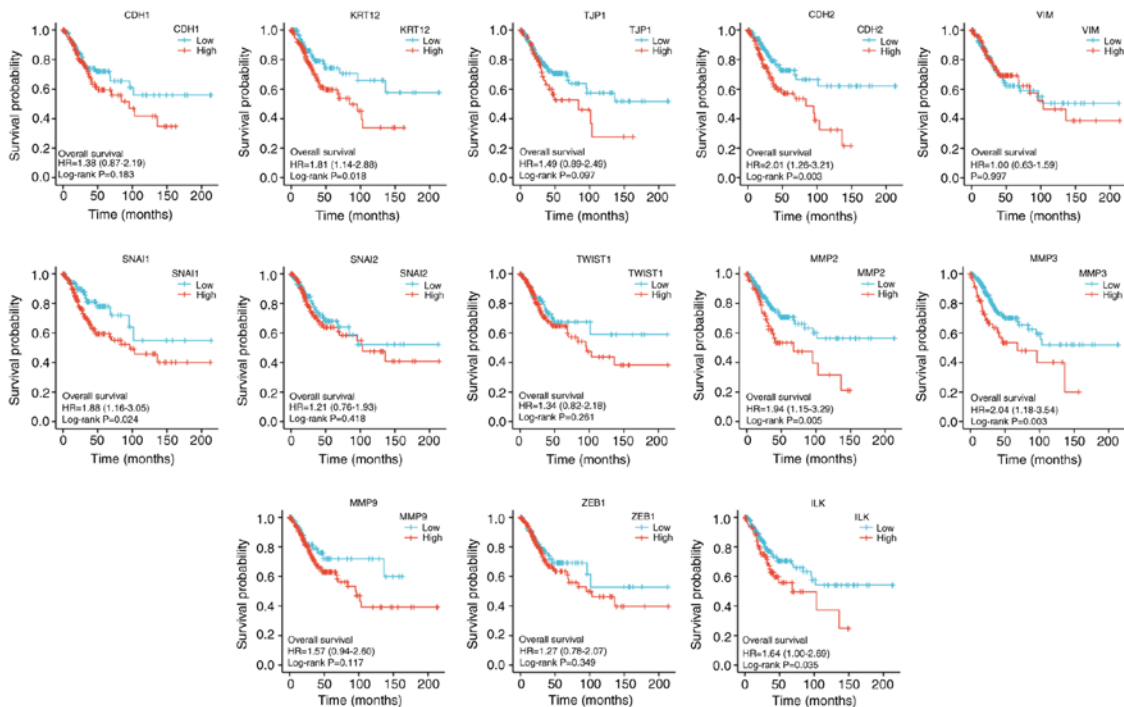


Figure 13. Kaplan-Meier overall survival curves according to high and low expression of CDH1, KRT12, TJP1, CDH2, VIM, SNAI1, SNAI2, TWIST1, MMP2, MMP3, MMP9, ZEB1, and ILK in cervical squamous cell carcinoma and adenocarcinoma samples tumor immune microenvironment. CDH1, E-cadherin; KRT12, cytokeratin 12; TJP1, tight junction protein 1; CDH2, N-cadherin; VIM, vimentin; ZEB1, zinc finger E-box-binding homeobox 1; ILK, integrin-linked protein kinase; HR, hazard ratio.
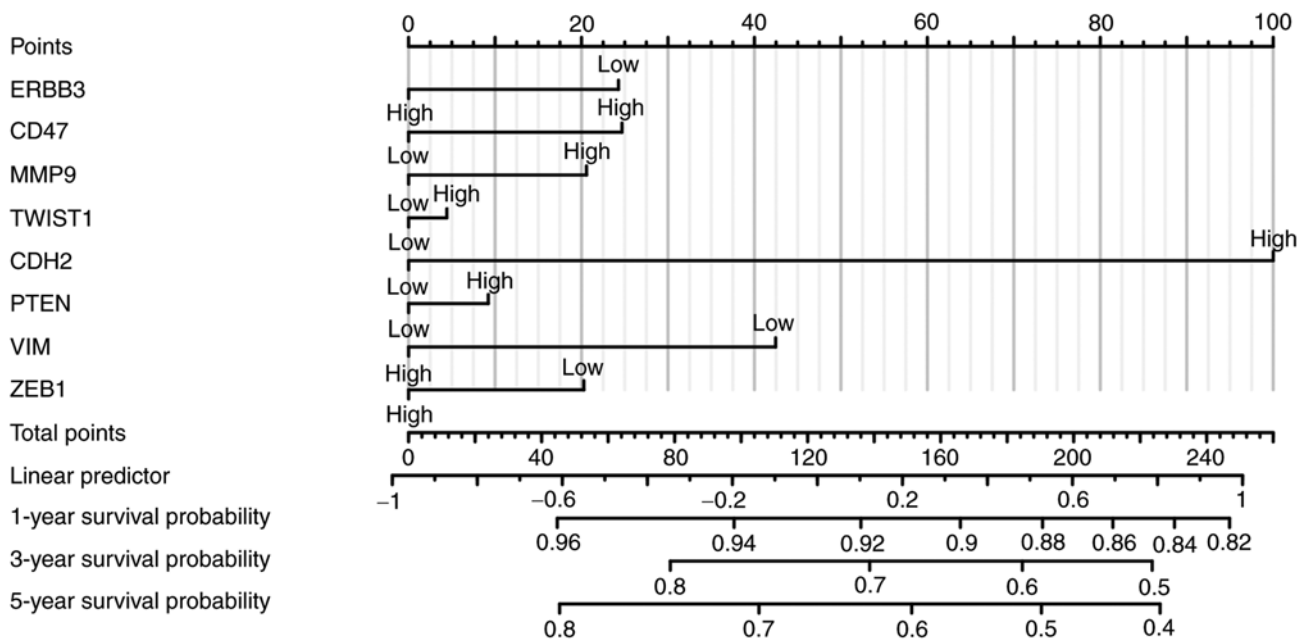
Figure 14. Multivariate model (nomogram chart of Cox regression) of cervical squamous cell carcinoma and adenocarcinoma for progression-free interval. CDH2, N-cadherin; VIM, vimentin; ZEB1, zinc finger E-box-binding homeobox 1.
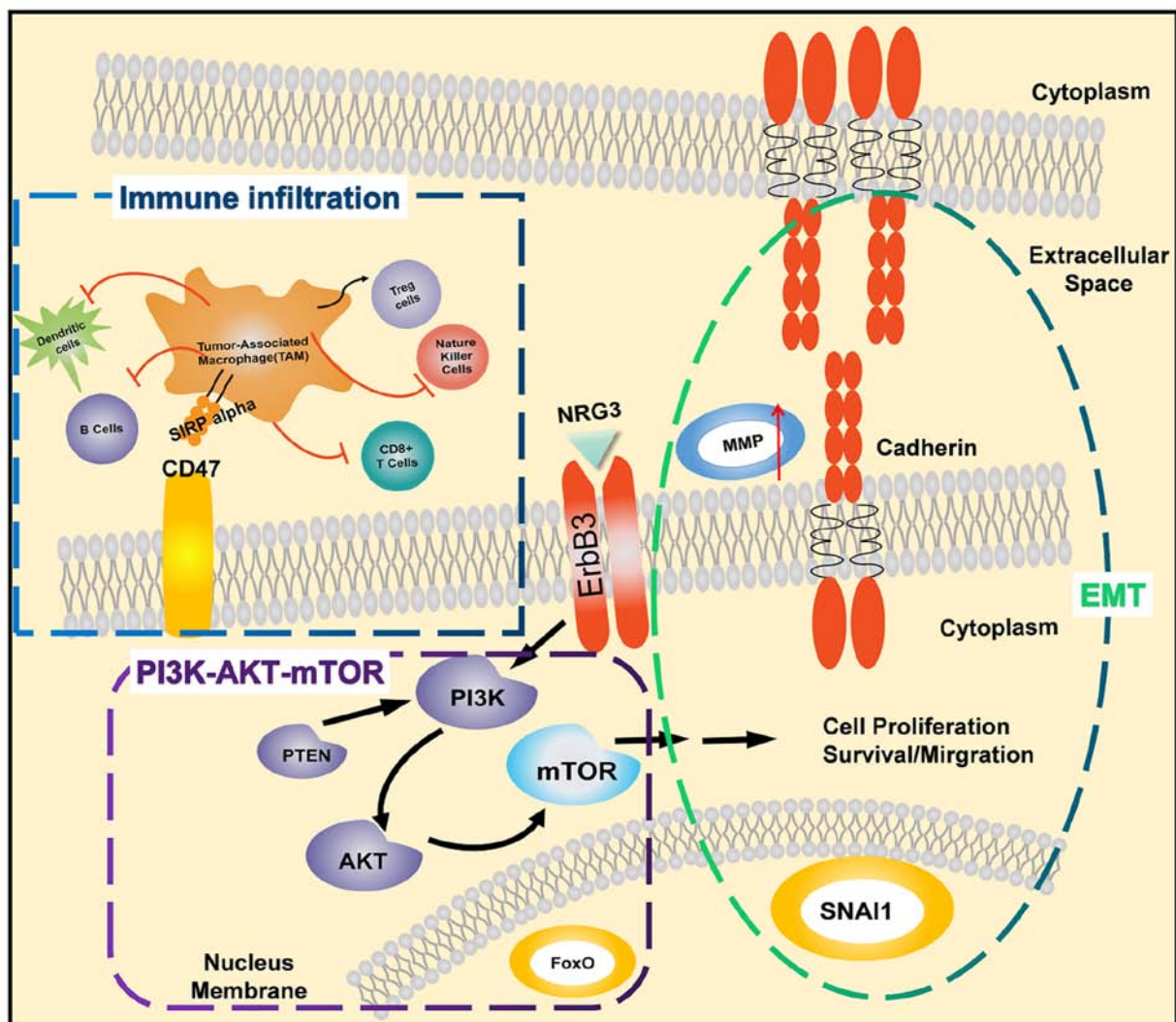


Figure 15. ERBB3-PI3K/AKT/mTOR pathway mediates the change of epithelial-mesenchymal transition status of cancer cells and contributes to the tumor immune microenvironment.

required for these features. In particular, simple MMP changes are not a prognostic factor in cervical cancer. When ERBB3 activates the PI3K pathway to change immune cell infiltration, the cervical cancer prognosis model is meaningful.

## Availability of data and materials

The datasets generated and analyzed during the current study are available in the cervical squamous cell carcinoma and endocervical adenocarcinoma (CESC) data in TCGA (https://portal.gdc.cancer.gov/). The datasets used and/or analyzed during the current study are available from the corresponding author on reasonable request.

## Authors' contributions

XY performed the data analysis work and aided in writing the manuscript. WZ designed the study and edited the manuscript. XY and WZ confirm the authenticity of all the raw data. All authors have read and approved the final manuscript.

## Ethics approval and consent to participate

Not applicable.

## Patient consent for publication

Not applicable.

## Competing interests

The authors declare that they have no competing interests.

## References

1. Cohen PA, Jhingran A, Oaknin A and Denny L: Cervical cancer. Lancet 393: 169-182, 2019.

2. Yugawa T and Kiyono T: Molecular mechanisms of cervical carcinogenesis by high-risk human papillomaviruses: Novel functions of E6 and E7 oncoproteins. Rev Med Virol 19: 97-113, 2009.

3. Zhang L, Wu J, Ling MT, Zhao L and Zhao KN: The role of the PI3K/Akt/mTOR signalling pathway in human cancers induced by infection with human papillomaviruses. Mol Cancer 14: 87, 2015.

4. Bossler F, Hoppe-Seyler K and Hoppe-Seyler F: PI3K/AKT/mTOR signaling regulates the virus/host cell crosstalk in HPV-positive cervical cancer cells. Int J Mol Sci 20: 2188, 2019.

5. Shi X, Wang J, Lei Y, Cong C, Tan D and Zhou X: Research progress on the PI3K/AKT signaling pathway in gynecological cancer. Mol Med Rep 19: 4529-4535, 2019.

6. Senga SS and Grose RP: Hallmarks of cancer-the new testament. Open Biol 11: 200358, 2021.

7. O'Donnell JS, Teng MWL and Smyth MJ: Cancer immunoediting and resistance to T cell-based immunotherapy. Nat Rev Clin Oncol 16: 151-167, 2019.

8. Fukumura D, Kloepper J, Amoozgar Z, Duda DG and Jain RK: Enhancing cancer immunotherapy using antiangiogenics: Opportunities and challenges. Nat Rev Clin Oncol 15: 325-340, 2018.

9. Aiello NM and Kang Y: Context-dependent EMT programs in cancer metastasis. J Exp Med 216: 1016-1026, 2019.

10. Taki M, Abiko K, Ukita M, Murakami R, Yamanoi K, Yamaguchi K, Hamanishi J, Baba T, Matsumura N and Mandai M: Tumor immune microenvironment during epithelial-mesenchymal transitionthe review of the loop between EMT and immunosuppression. Clin Cancer Res 27: 4669-4679, 2021.

11. Dongre A, Rashidian M, Reinhardt F, Bagnato A, Keckesova Z, Ploegh HL and Weinberg RA: Epithelial-to-mesenchymal transition contributes to immunosuppression in breast carcinomas. Cancer Res 77: 3982-3989, 2017.

12. Hoxhaj G and Manning BD: The PI3K-AKT network at the interface of oncogenic signalling and cancer metabolism. Nat Rev Cancer 20: 74-88, 2020.

13. Coussy F, El Botty R, Lavigne M, Gu C, Fuhrmann L, Briaux A, de Koning L, Dahmani A, Montaudon E, Morisset L, et al: Combination of PI3K and MEK inhibitors yields durable remission in PDX models of PIK3CA-mutated metaplastic breast cancers. J Hematol Oncol 13: 13, 2020.

14. Li M, Liu F, Zhang F, Zhou W, Jiang X, Yang Y, Qu K, Wang Y, Ma Q, Wang T, et al: Genomic ERBB2/ERBB3 mutations promote PD-L1-mediated immune escape in gallbladder cancer: a whole-exome sequencing analysis. Gut 68: 1024-1033, 2019.

15. Ross JS, Fakih M, Ali SM, Elvin JA, Schrock AB, Suh J, Vergilio JA, Ramkissoon S, Severson E, Daniel S, et al: Targeting HER2 in colorectal cancer: The landscape of amplification and short variant mutations in ERBB2 and ERBB3. Cancer 124: 1358-1373, 2018.

16. Van Lengerich B, Agnew C, Puchner EM, Huang B and Jura N: EGF and NRG induce phosphorylation of HER3/ERBB3 by EGFR using distinct oligomeric mechanisms. Proc Natl Acad Sci USA 114: E2836-E2845, 2017.

17. Sithanandam G and Anderson LM: The ERBB3 receptor in cancer and cancer gene therapy. Cancer Gene Ther 15: 413-448, 2008.

18. Moghbeli M, Makhdoumi Y, Delgosha MS, Aarabi A, Dadkhah E, Memar B, Abdollahi A and Abbaszadegan MR: ErbB1 and ErbB3 co-over expression as a prognostic factor in gastric cancer. Biol Res 52: 2, 2008.

19. Shi DM, Li LX, Bian XY, Shi XJ, Lu LL, Zhou HX, Pan TJ, Zhou J, Fan J and Wu WZ: miR-296-5p suppresses EMT of hepatocellular carcinoma via attenuating NRG1/ERBB2/ERBB3 signaling. J Exp Clin Cancer Res 37: 294, 2018.

20. Vivian J, Rao AA, Nothaft FA, Ketchum C, Armstrong J, Novak A, Pfeil J, Narkizian J, Deran AD, Musselman-Brown A, et al: Toil enables reproducible, open source, big biomedical data analyses. Nat Biotechnol 35: 314-316, 2017.

21. Yang J, Antin P, Berx G, Blanpain C, Brabletz T, Bronner M, Campbell K, Cano A, Casanova J, Christofori G, et al: EMT International Association (TEMTIA). Guidelines and definitions for research on epithelial-mesenchymal transition. Nat Rev Mol Cell Biol 21: 341-352, 2020.

22. Den Boon JA, Pyeon D, Wang SS, Horswill M, Schiffman M, Sherman M, Zuna RE, Wang Z, Hewitt SM, Pearson R, et al: Molecular transitions from papillomavirus infection to cervical precancer and cancer: Role of stromal estrogen receptor signaling. Proc Natl Acad Sci USA 112: E3255-E3264, 2015.

23. Scotto L, Narayan G, Nandula SV, Arias-Pulido H, Subramaniyam S, Schneider A, Kaufmann AM, Wright JD, Pothuri B, Mansukhani M and Murty VV: Identification of copy number gain and overexpressed genes on chromosome arm 20q by an integrative genomic approach in cervical cancer: Potential role in progression. Genes Chromosomes Cancer 47: 755-765, 2008.

24. Edgar R, Domrachev M and Lash AE: Gene expression omnibus: NCBI gene expression and hybridization array data repository. Nucleic Acids Res 30: 207-210, 2002.

25. Barrett T, Wilhite SE, Ledoux P, Evangelista C, Kim IF, Tomashevsky M, Marshall KA, Phillippy KH, Sherman PM, Holko M, et al: NCBI GEO: Archive for functional genomics data sets-update. Nucleic Acids Res 41: D991-D995, 2013.

26. Smyth GK: Limma: Linear models for microarray data. Bioinformatics and computational biology solutions using R and Bioconductor. Springer, New York, NY, 2005. 397-420.

27. Gu Z, Eils R and Schlesner M: Complex heatmaps reveal patterns and correlations in multidimensional genomic data. Bioinformatics 32: 2847-2849, 2016.

28. Bindea G, Mlecnik B, Tosolini M, Kirilovsky A, Waldner M, Obenauf AC, Angell H, Fredriksen T, Lafontaine L, Berger A, et al: Spatiotemporal dynamics of intratumoral immune cells reveal the immune landscape in human cancer. Immunity 39: 782-795, 2013.

29. Walter W, Sánchez-Cabo F and Ricote M: GOplot: An R package for visually combining expression data with functional analysis. Bioinformatics 31: 2912-2914, 2015.

30. Kanehisa M, Araki M, Goto S, Hattori M, Hirakawa M, Itoh M, Katayama T, Kawashima S, Okuda S, Tokimatsu T and Yamanishi Y: KEGG for linking genomes to life and the environment. Nucleic Acids Res 36(Database issue): D480-D484, 2007.

31. Yu G, Wang LG, Han Y and He QY: clusterProfiler: An R package for comparing biological themes among gene clusters. OMICS 16: 284-287, 2012.

32. Livak KJ and Schmittgen TD: Analysis of relative gene expression data using real-time quantitative PCR and the 2(-Delta Delta C(T)) method. Methods 25: 402-408, 2001.

33. Lanczky A and Gyorffy B: Web-based survival analysis tool tailored for medical research (KMplot): Development and implementation. J Med Internet Res 23: e27633, 2021.

34. Liu J, Lichtenberg T, Hoadley KA, Poisson LM, Lazar AJ, Cherniack AD, Kovatich AJ, Benz CC, Levine DA, Lee AV, et al: An integrated TCGA pan-cancer clinical data resource to drive high-quality survival outcome analytics. Cell 173: 400-416.e11, 2018.

35. Goel AL and Wu SM: Determination of ARL and a contour nomogram for CUSUM charts to control normal mean. Technometrics 13: 221-230, 1971.

36. Han H, Cho JW, Lee S, Yun A, Kim H, Bae D, Yang S, Kim CY, Lee M, Kim E, et al: TRRUST v2: An expanded reference database of human and mouse transcriptional regulatory interactions. Nucleic Acids Res 46: D380-D386, 2018.

37. R Core Team: A language and environment for statistical computing. R Foundation for Statistical Computing, Vienna, 2013. http://www.R-project.org/

38. Jeppson H and Hofmann H: Generalized Mosaic Plots in the ggplot2 Framework: Exploratory analysis of high-dimensional data with visual tools 17, 2021. https://rdrr.io/cran/ggmosaic/

39. Csardi G and Nepusz T: The igraph software package for complex network research. InterJournal Complex Systems 1695: 1-9, 2006.

40. Gustavsson E K, Zhang D, Reynolds R H, et al: ggtranscript: an R package for the visualization and interpretation of transcript isoforms using ggplot2. Bioinformatics 38(15): 3844-3846, 2022.

41. Kassambara A, Kosinski M and Biecek P: Package 'survminer'. Drawing Survival Curves using 'ggplot2'(R package version 03 1), 2017.

42. Cancer Genome Atlas Research Network: Integrated genomic and molecular characterization of cervical cancer. Nature 543: 378-384, 2017.

43. Yang X, Chen Y, Li M and Zhu W: ERBB3 methylation and immune infiltration in tumor microenvironment of cervical cancer. Sci Rep 12: 8112, 2022.

44. Soto D, Song C and McLaughlin-Drubin ME: Epigenetic alterations in human papillomavirus-associated cancers. Viruses 9: 248, 2017.

45. Senapati R, Senapati NN and Dwibedi B: Molecular mechanisms of HPV mediated neoplastic progression. Infect Agent Cancer 11: 59, 2016.

46. Narisawa-Saito M and Kiyono T: Basic mechanisms of high-risk human papillomavirus-induced carcinogenesis: Roles of E6 and E7 proteins. Cancer Sci 98: 1505-1511, 2007.

47. Martinez-Zapien D, Ruiz FX, Poirson J, Mitschler A, Ramirez J, Forster A, Cousido-Siah A, Masson M, Pol SV, Podjarny A, et al: Structure of the E6/E6AP/p53 complex required for HPV-mediated degradation of p53. Nature 529: 541-545, 2016.

48. Karamanou K, Franchi M, Vynios D and Brézillon S: Epithelial-to-mesenchymal transition and invadopodia markers in breast cancer: Lumican a key regulator. Semin Cancer Biol 62: 125-133, 2020.

49. Yang HL, Thiyagarajan V, Shen PC, Mathew DC, Lin KY, Liao JW and Hseu YC: Anti-EMT properties of CoQ0 attributed to PI3K/AKT/NFKB/MMP-9 signaling pathway through ROS-mediated apoptosis. J Exp Clin Cancer Res 38: 186, 2019.

50. Mao X, Xu J, Wang W, Liang C, Hua J, Liu J, Zhang B, Meng Q, Yu X and Shi S: Crosstalk between cancer-associated fibroblasts and immune cells in the tumor microenvironment: New findings and future perspectives. Mol Cancer 20: 131, 2021.

51. Looi CK, Chung FFL, Leong CO, Wong SF, Rosli R and Mai SW: Therapeutic challenges and current immunomodulatory strategies in targeting the immunosuppressive pancreatic tumor microenvironment. J Exp Clin Cancer Res 38: 162, 2019.

52. Cheng YQ, Wang SB, Liu JH, Jin L, Liu Y, Li CY, Su YR, Liu YR, Sang X, Wan Q, et al: Modifying the tumour microenvironment and reverting tumour cells: New strategies for treating malignant tumours. Cell Prolif 53: e12865, 2020.

53. Li D and Wu M: Pattern recognition receptors in health and diseases. Signal Transduct Target Ther 6: 291, 2021.

54. Mendes F, Domingues C, Rodrigues-Santos P, Abrantes AM, Gonçalves AC, Estrela J, Encarnação J, Pires AS, Laranjo M, Alves V, et al: The role of immune system exhaustion on cancer cell escape and anti-tumor immune induction after irradiation. Biochim Biophys Acta 1865: 168-175, 2016.

55. Liu Y and Cao X: Immunosuppressive cells in tumor immune escape and metastasis. J Mol Med (Berl) 94: 509-522, 2016.

56. Che Y, Yang Y, Suo J, An Y and Wang X: Induction of systemic immune responses and reversion of immunosuppression in the tumor microenvironment by a therapeutic vaccine for cervical cancer. Cancer Immunol Immunother 69: 2651-2664, 2020.

57. Jayshree RS: The immune microenvironment in human papilloma virus-induced cervical lesions-evidence for estrogen as an immunomodulator. Front Cell Infect Microbiol 11: 649815, 2021.

58. Welters MJ, van der Sluis TC, van Meir H, Loof NM, van Ham VJ, van Duikeren S, Santegoets SJ, Arens R, de Kam ML, Cohen AF, et al: Vaccination during myeloid cell depletion by cancer chemotherapy fosters robust T cell responses. Sci Transl Med 8: 334ra52, 2016.

59. Todd RW, Roberts S, Mann CH, Luesley DM, Gallimore PH and Steele JC: Human papillomavirus (HPV) type 16-specific CD8+ T cell responses in women with high grade vulvar intraepithelial neoplasia. Int J Cancer 108: 857-862, 2004.

60. Torres-Poveda K, Bahena-Román M, Madrid-González C, Burguete-García AI, Bermúdez-Morales VH, Peralta-Zaragoza O and Madrid-Marina V: Role of IL-10 and TGF-β1 in local immunosuppression in HPV-associated cervical neoplasia. World J Clin Oncol 5: 753-763, 2014.

61. Kalathil SG and Thanavala Y: High immunosuppressive burden in cancer patients: A major hurdle for cancer immunotherapy. Cancer Immunol Immunother 65: 813-819, 2016.

62. Huang YK, Wang M, Sun Y, Di Costanzo N, Mitchell C, Achuthan A, Hamilton JA, Busuttil RA and Boussioutas A: Macrophage spatial heterogeneity in gastric cancer defined by multiplex immunohistochemistry. Nat Commun 10: 3928, 2019.

63. Zhang Y and Zhang Z: The history and advances in cancer immunotherapy: Understanding the characteristics of tumor-infiltrating immune cells and their therapeutic implications. Cell Mol Immunol 17: 807-821, 2020.

64. Chao MP, Weissman IL and Majeti R: The CD47-SIRPα pathway in cancer immune evasion and potential therapeutic implications. Curr Opin Immunol 24: 225-232, 2012.

65. Feng M, Jiang W, Kim BYS, Zhang CC, Fu YX and Weissman IL: Phagocytosis checkpoints as new targets for cancer immunotherapy. Nat Rev Cancer 19: 568-586, 2019.

66. Oronsky B, Carter C, Reid T, Brinkhaus F and Knox SJ: Just eat it: A review of CD47 and SIRP-α antagonism. Semin Oncol 47: 117-124, 2020.

67. Li Z, Li Y, Gao J, Fu Y, Hua P, Jing Y, Cai M, Wang H and Tong T: The role of CD47-SIRPα immune checkpoint in tumor immune evasion and innate immunotherapy. Life Sci 273: 119150, 2021.
68. Huang CY, Ye ZH, Huang MY and Lu JJ: Regulation of CD47 expression in cancer cells. Transl Oncol 13: 100862, 2020.
69. Yang H, Shao R, Huang H, Wang X, Rong Z and Lin Y: Engineering macrophages to phagocytose cancer cells by blocking the CD47/SIRPα axis. Cancer Med 8: 4245-4253, 2019.
70. Braicu EI, Gasimli K, Richter R, Nassir M, Kümmel S, Blohmer JU, Yalcinkaya I, Chekerov R, Ignat I, Ionescu A, et al: Role of serum VEGFA, TIMP2, MMP2 and MMP9 in monitoring response to adjuvant radiochemotherapy in patients with primary cervical cancer-results of a companion protocol of the randomized NOGGO-AGO phase III clinical trial. Anticancer Res 34: 385-391, 2014.
71. Riani M, Le Jan S, Plée J, Durlach A, Le Naour R, Haegeman G, Bernard P and Antonicelli F: Bullous pemphigoid outcome is associated with CXCL10-induced matrix metalloproteinase 9 secretion from monocytes and neutrophils but not lymphocytes. J Allergy Clin Immunol 139: 863-872.e3, 2017.
72. Yi W, Tu MJ, Liu Z, Zhang C, Batra N, Yu AX and Yu AM: Bioengineered miR-328-3p modulates GLUT1-mediated glucose uptake and metabolism to exert synergistic antiproliferative effects with chemotherapeutics. Acta Pharm Sin B 10: 159-170, 2020.
73. Vasconcelos RC, de Oliveira Moura JM, Junior VLB, da Silveira ÉJ and de Souza LB: Immunohistochemical expression of GLUT-1, GLUT-3, and carbonic anhydrase IX in benign odontogenic lesions. J Oral Pathol Med 45: 712-717, 2016.
74. Cheng SC, Quintin J, Cramer RA, Shepardson KM, Saeed S, Kumar V, Giamarellos-Bourboulis EJ, Martens JH, Rao NA, Aghajanirefah A, et al: mTOR- and HIF-1α-mediated aerobic glycolysis as metabolic basis for trained immunity. Science 345: 1250684, 2014.
75. Giovanelli P, Sandoval TA and Cubillos-Ruiz JR: Dendritic cell metabolism and function in tumors. Trends Immunol 40: 699-718, 2019.
76. Kim IS and Zhang XHF: One microenvironment does not fit all: Heterogeneity beyond cancer cells. Cancer Metastasis Rev 35: 601-629, 2016.
77. Sobral-Leite M, Salomon I, Opdam M, Kruger DT, Beelen KJ, van der Noort V, van Vlierberghe RLP, Blok EJ, Giardiello D, Sanders J, et al: Cancer-immune interactions in ER-positive breast cancers: PI3K pathway alterations and tumor-infiltrating lymphocytes. Breast Cancer Res 21: 90, 2019.
78. Rivera LB, Meyronet D, Hervieu V, Frederick MJ, Bergsland E and Bergers G: Intratumoral myeloid cells regulate responsiveness and resistance to antiangiogenic therapy. Cell Rep 11: 577-591, 2015.
79. Lambertz U, Silverman JM, Nandan D, McMaster WR, Clos J, Foster LJ and Reiner NE: Secreted virulence factors and immune evasion in visceral leishmaniasis. J Leukoc Biol 91: 887-899, 2012.
80. Crane CA, Panner A, Murray JC, Wilson SP, Xu H, Chen L, Simko JP, Waldman FM, Pieper RO and Parsa AT: PI (3) kinase is associated with a mechanism of immunoresistance in breast and prostate cancer. Oncogene 28: 306-312, 2009.
81. Bahrami A, Hasanzadeh M, Hassanian SM, ShahidSales S, Ghayour-Mobarhan M, Ferns GA and Avan A: The potential value of the PI3K/Akt/mTOR signaling pathway for assessing prognosis in cervical cancer and as a target for therapy. J Cell Biochem 118: 4163-4169, 2017.
82. Chai J, Modak C, Mouazzen W, Narvaez R and Pham J: Epithelial or mesenchymal: Where to draw the line? Biosci Trends 4: 130-142, 2010.
83. Gerber TS, Ridder DA, Schindeldecker M, Weinmann A, Duret D, Breuhahn K, Galle PR, Schirmacher P, Roth W, Lang H and Straub BK: Constitutive occurrence of E: N-cadherin heterodimers in adherens junctions of hepatocytes and derived tumors. Cells 11: 2507, 2022.
84. Deshmukh AP, Vasaikar SV, Tomczak K, Tripathi S, den Hollander P, Arslan E, Chakraborty P, Soundararajan R, Jolly MK, Rai K, et al: Identification of EMT signaling cross-talk and gene regulatory networks by single-cell RNA sequencing. Proc Natl Acad Sci USA 118: e2102050118, 2021.
85. Suarez-Carmona M, Lesage J, Cataldo D and Gilles C: EMT and inflammation: Inseparable actors of cancer progression. Mol Oncol 11: 805-823, 2017.